This is a "preproof" accepted article for *Journal of Glaciology*.
This version may be subject to change during the production process.
10.1017/jog.2025.37

Retreat and Frontal Ablation Rates for Alaska's Lake-Terminating Glaciers: Investigating Potential Physical Controls with Implications for Future Stability

Noah G. Caldwell[1], William H Armstrong[1,*], Robert McNabb[2], Ellyn M. Enderlin[3], Daniel McGrath[4], Brianna Rick[5], Jacob Hanson[1], and L. Baker Perry[1,6]

[1]Department of Geological and Environmental Sciences, Appalachian State University, Boone, NC USA
[2]School of Geography and Environmental Sciences, Ulster University, Coleraine, UK
[3]Department of Geoscience, Boise State University, Boise, ID USA
[4]Department of Geosciences, Colorado State University, Fort Collins, CO, USA
[5]Alaska Climate Adaptation Science Center, Fairbanks, AK, USA
[6]Department of Geography, University of Nevada Reno, Reno, NV, USA

Corresponding author: William H Armstrong Email: armstrongwh@appstate.edu

Abstract

Globally, glaciers are changing in response to climate warming, with those that terminate in water often undergoing the most rapid change. In Alaska and northwest Canada, proglacial lakes have grown in number and size but their influence on glacier mass loss is unclear. We characterized the rates of retreat and mass loss through frontal ablation of 55 lake-terminating glaciers (>14,000 $km^{2)}$ in the region using annual Landsat imagery from 1984 – 2021. We find a median retreat rate of 60 m a^{-1} (interquartile range = 35 – 89 m a^{-1}) over 1984 – 2018 and a median loss of 0.04 Gt a^{-1} (0.01 – 0.15 Gt a^{-1}) mass through frontal ablation over 2009 – 2018. Summed over 2009 – 2018, our study glaciers lost 6.1 Gt a^{-1} to frontal ablation. Analysis of bed profiles suggest that glaciers terminating in larger lakes and deeper water lose more mass to frontal ablation, and that the glaciers will remain lake-terminating for an average of 74 years (38 – 177 a). This work suggests that as more proglacial lakes form and as lakes become larger, enhanced frontal ablation could cause higher mass losses, which should be considered when projecting the future of lake-terminating glaciers.

1. Introduction

Mountain glaciers comprise 1% of global glacier ice volume yet account for ~1/3 of modern global sea level rise (Hugonnet and others, 2021). Of these glaciers, those that terminate in water show the largest changes in response to global warming, often due to abrupt collapses of the glacier tongue (Truffer and Motyka, 2016). Ongoing global glacier retreat has led to an increase in the number and size of proglacial lakes (Zhang and others, 2024), here defined as

https://doi.org/10.1017/jog.2025.37 Published online by Cambridge University Press

freshwater lakes in direct contact with ice at the glacier terminus. Glaciers that terminate in the ocean (marine-terminating glaciers) are known to undergo rapid and irreversible retreat (Pfeffer, 2007), raising concern about the dynamical stability of lake-terminating glaciers (Carrivick and Tweed, 2013). Lake-terminating-glaciers have been observed to flow faster (Pronk and others, 2021; Main and others, 2023) and thin more rapidly than land-terminating glaciers (Minowa and others, 2021; King and others, 2019; Larsen and others, 2015), which is often interpreted to reflect the lakes driving enhanced velocity or mass loss. However, lake-terminating glaciers are thought to respond less sensitively to the presence of water at their termini than marine-terminating glaciers (Benn and others, 2007a; Minowa and others, 2023) because the rate of frontal ablation, the sum of subaqueous melt and calving at the glacier terminus, is expected to be lower in lacustrine settings (Truffer and Motyka, 2016). In marine environments, iceberg calving is enhanced in deeper waters where ice is more likely to float and fracture along planes of weakness (Brown and others, 1982; Benn and others, 2007a; Nick and others, 2010). Subaqueous melt in marine settings is often driven by buoyant subglacial meltwater discharge entraining warm ambient fjord water, with the potential for rapid melt due to water's high heat capacity and heat transfer coefficient (Truffer and Motyka, 2016). High rates of subaqueous melt may further enhance calving by undercutting the terminus. Thus, the lack of buoyancy-driven melt enhancement and replenishment of warm subsurface waters in lacustrine settings (Truffer and Motyka, 2016; Sugiyama and others, 2021) may result in far lower rates of frontal ablation for lake-terminating glaciers than their marine counterparts (Trüssel and others, 2013). However, lake-terminating glaciers more frequently exhibit persistent floating tongues, buoyancy-driven calving (Boyce and others, 2007; Trüssel and others, 2013; Minowa and others, 2023), and terminus "over-cutting" leading to underwater ice terraces (Robertson and others, 2017; Sugiyama and others, 2019), which may make their dominant frontal ablation processes somewhat dissimilar from temperate marine-terminating glaciers.

Frontal ablation is a substantial contributor to mass loss for marine-terminating glaciers across the world (Kochtitzky and others, 2022; Mouginot and others, 2019; Rignot and others, 2019), but the contribution of frontal ablation to the mass loss of the world's lake-terminating glaciers is largely unknown. In the only known regional study addressing lake-terminating glacier frontal ablation, the median contribution of frontal ablation to mass loss across 30 Patagonian lake-terminating glaciers was estimated to be 13%, with the proportion reaching 50%

https://doi.org/10.1017/jog.2025.37 Published online by Cambridge University Press

on some glaciers (Minowa and others, 2021). On a rapidly-retreating Alaska lake-terminating glacier, frontal ablation was estimated to account for 8 – 17% of mass loss (Trüssel and others, 2013). Despite the potential for a mechanism for additional mass loss, no regional estimate exists to constrain the magnitude of frontal ablation on Alaska's lake-terminating glaciers, nor its potential impact on glacier change.

Ice-marginal lakes (i.e., either proglacial, ice-dammed, or supraglacial) expanded rapidly in recent decades, with an increase in both number and areal extent of lakes documented from Patagonia (Wilson and others, 2018) to Greenland (How and others, 2021) and many areas in between (e.g., Chen and others, 2021; Mölg and others, 2021; Carrivick and others, 2022). Over 14,400 ice-marginal lakes now exist across the world, covering an area of 9,000 km^2 with a volume of 157 km^3 (Shugar and others, 2020). In Alaska, ice-marginal lakes grew approximately three times faster than the global average, with proglacial lakes increasing in area by 85% between 1984 – 2019 to now cover 1000 km^2 (Rick and others, 2022). The formation and drainage of proglacial lakes can have profound effects on the surrounding environment and downstream communities by altering suspended sediment flux and stream flow characteristics, creating habitats (Dorava and Milner, 2000), changing downstream water resources (Farinotti and others, 2019), and increasing risk of glacial lake outburst floods when a lake dam fails or is overtopped (Carrivick and Tweed, 2013; Rick and others, 2022; Veh and others, 2023). Proglacial lake growth should also influence rates of frontal ablation, as larger lakes have more surface area available to absorb solar radiation, resulting in warmer water temperatures and higher rates of subaqueous melt (Trüssel and others, 2013; Sugiyama and others, 2016). Larger lakes also tend to be deeper (Cook & Quincey, 2015), so lake growth may result in higher flotation fractions and more vigorous mass loss through calving.

This study provides new insight into freshwater frontal ablation processes by quantifying the retreat rates of Alaska's lake-terminating glaciers since 1984 using Landsat imagery and comparing retreat values with those found on Alaska marine-terminating glaciers (McNabb and others, 2015). Combining new satellite-derived terminus position observations and previously-published geospatial datasets (i.e., ice thickness and velocity), we use a mass conservation approach to estimate rates of frontal ablation on Alaska's lake terminating glaciers. We then explore associations between environmental variables (e.g., lake area, glacier area, estimated

https://doi.org/10.1017/jog.2025.37 Published online by Cambridge University Press

flotation fraction) and the observed retreat and frontal ablation rates. Lastly, we use existing geospatial datasets to estimate the time remaining for lake-terminating glaciers to retreat above the recent lake surface elevation, providing an estimate for when these glaciers will become land-terminating.

2. Methods

2.1 Study area

Our study focuses on Alaska and northwest Canada, a region where ice-marginal lakes grew three times faster than the global average between 1990 and 2018 (Shugar and others, 2020). The region's proglacial lakes grew faster than other types of ice-marginal lakes (e.g., ice-dammed or supraglacial lakes), increasing in area by 85% (543 km^2 to 1006 km^2) between 1984 and 2019 (Rick and others, 2022). This rapid expansion of proglacial lakes coincides with accelerated loss of glacial ice in the Alaska-British Columbia-Yukon region (Randolph Glacier Inventory, RGI, Region 01), which had a mean surface lowering rate of 0.91 m a^{-1} between 2000 and 2019 (Hugonnet and others, 2021). The region's abundance of rapidly changing proglacial lakes makes it an ideal site to capture the range of behavior possible on lake-terminating glaciers.

Our study focuses on 55 lake-terminating glaciers covering ~14,000 km^2 and spanning 56–64° N and 130–154° W (Fig. 1). This dataset includes most of the lake-terminating glaciers in RGI Region 01 larger than 100 km^2, as well as the region's 14 most rapidly growing proglacial lakes that formed during the Landsat record (Rick and others, 2022), 8 of which are <100 km^2. We exclude several glaciers that the RGI defines as lake-terminating (RGI Region 01 IDs: 12425 – Triumvirate Glacier, 17348 – Russell Glacier, 20796 – Brady Glacier) because they lack true proglacial lakes. In these cases, ice-dammed or small proglacial lakes are found near the terminus, but the glaciers lack a large, coalesced lake downstream from the terminus. Our study glaciers cover 83% of all lake-terminating glacier area in RGI region 01 as defined by the RGI Version 6 (Figure S1). We focus on the larger lake-terminating glaciers from the RGI to facilitate higher quality ice thickness and velocity data. By adding the 14 fastest-growing new proglacial lakes from Rick and others (2022), we seek to provide an upper bound on lake-terminating glacier retreat and presumably frontal ablation rates.

https://doi.org/10.1017/jog.2025.37 Published online by Cambridge University Press

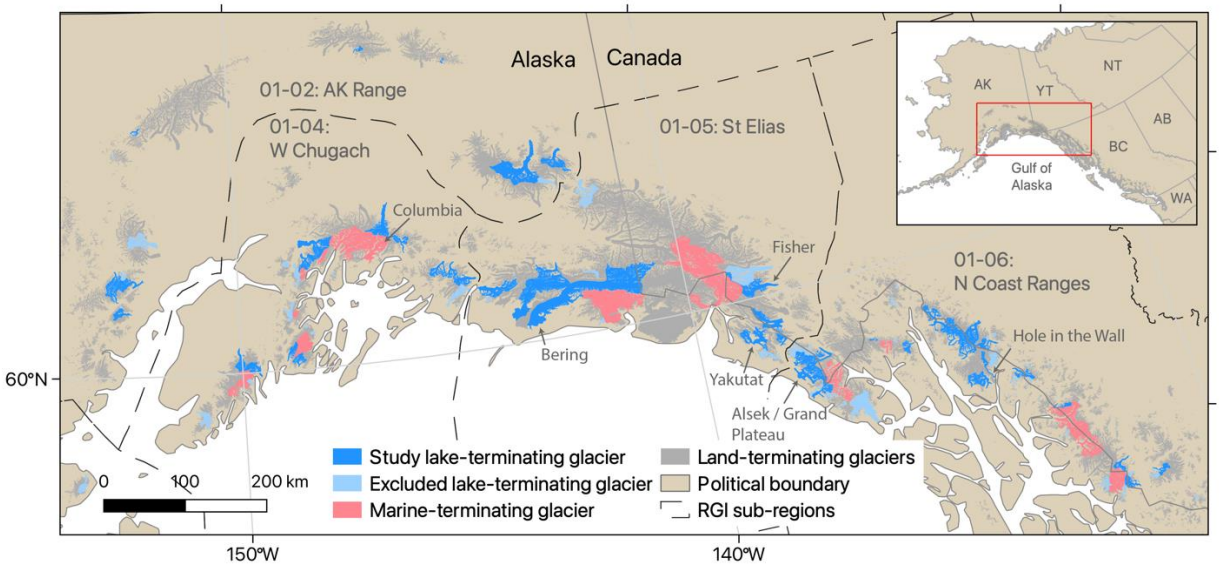

Figure 1. Distribution of study glaciers in Alaska and northwest Canada used for this research. Lake-terminating glaciers considered in this study (n=55) are shown in dark blue stars, with marine-terminating glaciers (n=27) from McNabb and others (2015) shown in pink. Light blue glaciers are classified as lake-terminating by the Randolph Glacier Inventory (RGI) v6 but were excluded from this study either due to the 100 km^2 glacier area minimum threshold or special circumstances described in the text. RGI region 01 sub-regions are delineated by black lines and labeled with gray text. Some minor discrepancies exist between the glacier outlines of McNabb and others (2015) and those shown here, which are from RGI Consortium (2017). Map is projected in Alaska Albers (EPSG:3338).

2.2 Quantifying glacier retreat rates

We use the Google Earth Engine Digitisation Tool (GEEDiT; Lea, 2018) to manually digitize glacier terminus positions with annual resolution from primarily melt season (May-September) Landsat imagery spanning 1984–2021. Length change time series are calculated using the single central flowline method provided by the Margin Change Quantification Tool (MaQIT; Fig. 2; Lea, 2018). We use the centerlines provided by the Open Global Glacier Model (Maussion and others, 2019; accessible at https://docs.oggm.org/en/stable/assets.html).

We assess temporal variations in retreat rate by calculating the average rate of length change over the entire study period as well as three approximately decadal periods: 1986 – 1998, 1999 – 2008, and 2009 – 2018. These time-periods align with the lake area delineations of Rick and others (2022), which allows us to investigate possible relationships between proglacial lake area and glacier retreat rate. For each glacier, we isolated length data in each period. Within that

https://doi.org/10.1017/jog.2025.37 Published online by Cambridge University Press

period, we obtained a linear fit to the data using the non-parametric Theil-Sen regression method (Helsel and others, 2020). Given the sparse number of observations for each time period, we used the Theil-Sen regression method because it is resistant to outliers and does not assume input data are normally distributed. The slope of the Theil-Sen fit line provides our estimate of average rate of length change during the period. While ordinary least squares regression would likely produce similar results for this analysis of changes in retreat rates, we employ Theil-Sen correlation here for methodological consistency with for our later analyses (Section 2.6) in which outlying data points would skew the overall statistical results provided by ordinary least squares.

There is short-term variability in retreat rates due to image timing and seasonality of retreat, but, as our study is focused on multi-decadal behavior, we neglect seasonal variations in retreat and frontal ablation. The middle 80% (10th - 90th percentiles) of our input imagery comes from days of year (DOYs) 132 – 274 (11 May - 30 Sept), with a median image DOY of 198 (16 July; Fig. S2).

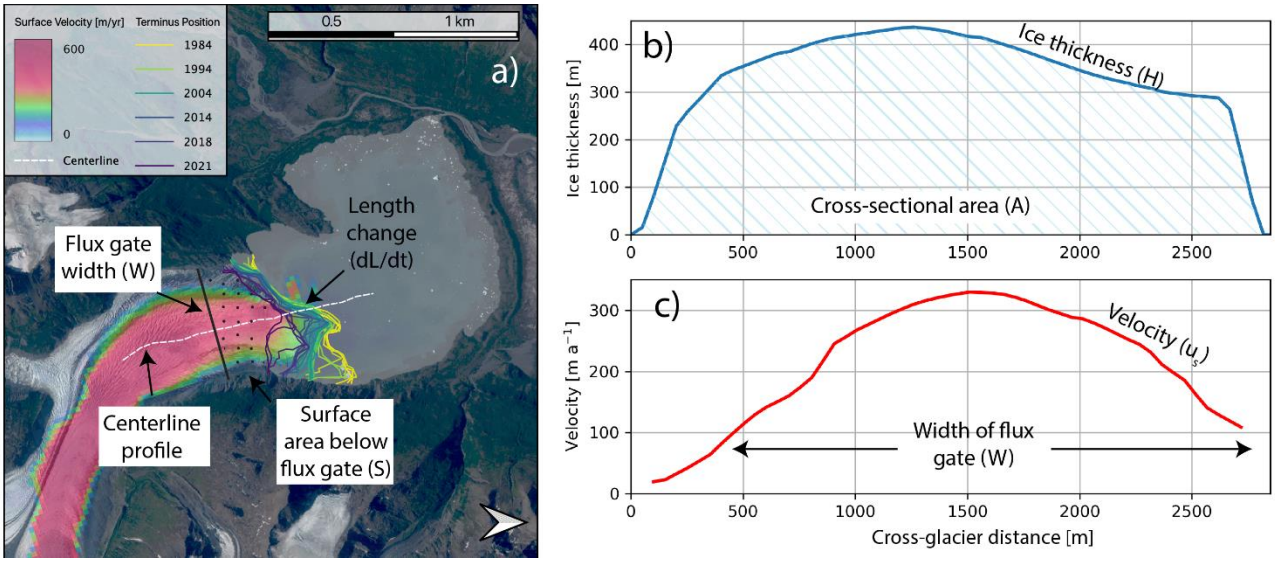

Figure 2. Physical overview of quantities used to estimate retreat and frontal ablation rates. (a) Surface velocity map of Colony Glacier (RGI60-01.10006). Digitized glacier terminus positions, measured annually using GEEDiT (Lea, 2018), are shown as lines with a gradient color scheme. The near terminus flux gate, set upstream of the furthest upstream terminus position, is used to calculate ice flux in and out of the near-terminus control volume. The surface area below cross section (*S*) is used to calculate mass loss from surface melt. (b) Ice thickness (line) and cross-sectional area (hatched area) used to calculate mass flux across flux gate with the addition of (c) ice surface velocity and width of flux gate. Ice thickness and surface velocity data are from Millan and others (2022). Background image in (a) is a 2018 Sentinel-2 image.

https://doi.org/10.1017/jog.2025.37 Published online by Cambridge University Press

2.3 Estimating rates of frontal ablation

Following the approach of McNabb and others (2015), we estimate frontal ablation rates by first defining mass conservation below a near-terminus flux gate, given as:

$$\underbrace{A\frac{dL}{dt}}_{Q_{ret}} = \underbrace{\gamma \int_0^W H(y)\, u_s(y) \cdot \hat{n}\, dy}_{Q_{in}} - F + \underbrace{\dot{b}S}_{Q_{melt}} \quad \textbf{(1)}$$

LATEX COMMAND FOR THIS EQUATION:

\[
\underbrace{A \frac{\text{d}L}{\text{d}t}}_{Q_{ret}} =
\underbrace{\gamma \int_0^W H(y) u_s(y) \cdot \hat{n} \text{ d}y}_{Q_{in}} - F +
\underbrace{\dot{b}S}_{Q_{melt}}
\]

where A is the cross-sectional area of the near-terminus flux gate estimated from the Millan and others (2022) modeled ice thickness estimates, $\frac{dL}{dt}$ is the Theil-Sen slope-estimated retreat rate, γ is a parameter that scales the surface velocity to column-averaged velocity, and H and u_s are respectively modeled ice thickness and remotely sensed ice surface velocity from Millan and others (2022). W is glacier width, y is the flow-transverse coordinate, $\hat{n}$ is the vector normal to the flux gate, F is the frontal ablation rate, $\dot{b}$ is the assumed surface mass balance, and S is the glacier's surface area between the flux gate and terminus (Fig. 2a). Flux gate locations were chosen to be as close to the modern terminus position as possible while maintaining physically plausible surface velocity and ice thickness data, which often decline in quality towards the terminus. Conceptually, the left-hand side of (1) represents mass change in the "control volume" below the flux gate due to advance or retreat (Q_{ret}), which is set by the balance of mass gain due to ice flow across the flux gate (first term on right-hand side; Q_{in}) and mass loss through frontal ablation (F) and surface melt (the third terms on right-hand side; Q_{melt}). Basal velocities are generally high near calving fronts (Cuffey and Paterson, 2010) and we set $\gamma = 0.9$ reflecting roughly equal contributions of basal motion and internal deformation to glacier surface velocity. Following McNabb and others (2015), we assume a high estimate of –10 m a^{-1} for surface mass balance ($\dot{b}$), which matches the most negative surface mass balance value found near the terminus of a single marine-terminating glacier (Columbia Glacier; Rasmussen and others,

https://doi.org/10.1017/jog.2025.37 Published online by Cambridge University Press

2011). We stress that this assumed value of $\dot{b}$ is not applied over the glacier's entire area but only applied over the relatively small surface area below the flux gate (*S*; Fig. 2a). Using a high estimate of surface mass balance and an intermediate value for γ yields conservative (i.e., low) estimates of frontal ablation and is consistent with the methodology of McNabb and others (2015), facilitating direct comparison of our estimates. We note that, by convention, negative $\frac{dL}{dt}$ indicates glacier retreat, positive Q_{in} indicates mass gain, positive *F* represents mass loss through frontal ablation, and $\dot{b}$ corresponds to surface melt. Rearranging (1) to solve for frontal ablation (*F*), we have**:**

$$F = Q_{in} - Q_{ret} + Q_{melt} = \gamma \int_0^W H(y)\, u_s(y) \cdot \hat{n}\, dy - A\frac{dL}{dt} + \dot{b}S \qquad \textbf{(2)}$$

where all terms have been defined previously (Table S1).

Unless otherwise stated, all estimate of frontal ablation below use $\frac{dL}{dt}$ from 2009 – 2018, as it is the study sub-period that best aligns with the timing of the other input datasets. Surface velocities (u_s) in Millan and others (2022) reflect an average over 2017 – 2018, and associated thickness is estimated using a multitemporal DEM built from stereo imagery collected from ASTER (launched in 1999) and the WorldView constellation (first launched in 2007), with results computed over an average ~2010 glacier outline (RGI Consortium, 2017). Utilizing the slower average $\frac{dL}{dt}$ rates estimated over the whole 1984 – 2021 study period results in a median decrease in *F* of 0.001 Gt a^{-1}, with an interdecile range of –0.021 to 0.071 Gt a^{-1} (negative values indicate lower *F* using the 2009 – 2018 retreat rates, which would be produced by retreat rate slowing over time; Fig. S3).

2.4 Estimating uncertainty in frontal ablation

To estimate errors, we simplify Equation 2 into a cross-sectionally-averaged form,

$$F \approx \gamma \bar{H}\bar{u}W - \bar{H}W\frac{dL}{dt} + \dot{b}S \qquad \textbf{(3)}$$

where overbars indicate the average value across the cross-section. We estimate uncertainty in the first two terms, which respectively represent mass gained from ice flux across the flux gate (Q_{in}) and mass lost through terminus retreat (Q_{ret}), as described below. We assess the uncertainty of our estimates of *F* due to the assumed high-end plausible mass balance value ($\dot{b}$ = –10 m a^{-1})

https://doi.org/10.1017/jog.2025.37 Published online by Cambridge University Press

by recalculating F with $\dot{b}$ = –5 m a^{-1} and find a median F increase of 0.006 Gt a^{-1} (9%; Fig. S4). Importantly, a lower near-terminal surface melt rate results in higher estimated frontal ablation rates, so our results present a conservative (i.e., low) figure (described further in Section 2.3). The actual uncertainty due to the assumed surface mass balance below the flux gate is a systematic error of unknown magnitude, which we omit from the following error propagation, but the analysis above gives an idea of its relative magnitude.

Assuming error terms are independent and normally distributed, uncertainty in the incoming ice flux (δQ_{in}) is given as

$$\delta Q_{in} = Q_{in} \cdot \sqrt{\left(\frac{\delta\gamma}{\gamma}\right)^2 + \left(\frac{\delta H}{\underline{H}}\right)^2 + \left(\frac{\delta u}{\underline{u}}\right)^2 + \left(\frac{\delta W}{W}\right)^2} \quad \textbf{(4)}$$

where we use $\delta\gamma = 0.1$ and $\delta W = 60$ m (±1 pixel) as set values, with the remaining terms varying on a glacier-by-glacier basis. For δH and δu, we take the mean stated uncertainty (Millan and others, 2022) across the cross-section. In general, the ice thickness dataset differs from measurements within ±25% for ice thicker than 200 m (Figs. S3 and S9 in Millan and others, 2022). Radar observations for ground-truthing these estimates across Alaska remain sparse (Tober, 2023; Welty and others, 2020), but for the median flux gate ice thickness of 403 m across our study glaciers, the ±25% corresponds to approximately ± 100 m (Millan and others, 2022). Utilizing velocity data from 2017 – 2018 to compute frontal ablation rates over 2009 – 2018 relies on an implicit assumption that annual average velocity does not vary significantly over the longer time period. This assumption results in additional uncertainty in Q_{in} that cannot be estimated without outside knowledge of how representative the 2017 – 2018 velocity is for the 2009 – 2018 period, as well as how this varies across glaciers. We acknowledge this limitation but still utilize the dataset due to its widespread geographic coverage, well-quantified error, and ease of use. Ice thickness also represents a 2017 – 2018 snapshot in time, but systematic changes in ice thickness over 2009 – 2018 are likely small relative to the random error in the Milan and others (2022) ice thickness described above.

Uncertainty in Q_{ret} is calculated in a similar manner to that for $Q_{in}$and we then estimate uncertainty in frontal ablation (δF) as

https://doi.org/10.1017/jog.2025.37 Published online by Cambridge University Press

$$\delta F = \sqrt{(\delta Q_{in})^2 + (\delta Q_{ret})^2} \quad \textbf{(5)}$$

On average, δQ_{in} is 28% of Q_{in} and δQ_{ret} is 26% of Q_{ret}. Uncertainty in frontal ablation scales with the magnitude of frontal ablation, with an average uncertainty of 24% (Figure S5).

2.5 Comparison marine-terminating glacier data set

We compare our estimated rates of retreat and frontal ablation for lake-terminating glaciers with estimates for Alaska's marine-terminating glaciers from McNabb and others (2015). The McNabb dataset consists of 27 marine-terminating glaciers covering an area of ~11,000 km^2 (Fig. 1), while the 55 lake-terminating glaciers in this study cover ~14,000 km^2. These marine-terminating glaciers represent 96% of the total tidewater glacier area in Alaska, accounting for 12.6% of the total RGI Region 1 glacier area (McNabb and others, 2015). The marine-terminating dataset incorporates Landsat data spanning 1985 – 2013 with at least five observations of terminus positions per year on average and reported average uncertainties in retreat and frontal ablation of 10% and 24% respectively.

2.6 Investigating potential physical drivers and forecasting long-term change

We manually identified the lake surface elevation and extracted glacier centerline surface elevation (Z_s) profiles using the Copernicus 3 arc-second (GLO-90; ~90 m pixel) digital elevation model (European Space Agency, 2024). We utilize this dataset rather than a higher resolution time-stamped source like the ArcticDEM because lake elevation is often poorly resolved in this optical image-derived dataset, file sizes are large enough that data analysis becomes more cumbersome, and our analysis does not require fine spatial resolution. The GLO-90 DEM represents the land surface over 2011 – 2015 and covers the high latitudes with <4 m elevation uncertainty (European Space Agency, 2024). The dataset's survey date roughly corresponds with the modal 2010 glacier outline date for the Randolph Glacier Inventory in this region (RGI Consortium, 2017), which is an input to the Millan and others (2022) ice thickness dataset. We then estimated the glacier bed elevation (z_b; Fig. 3) by subtracting the Millan and others (2022) ice thickness from the GLO-90 surface elevation along the glacier centerline using profiles from Maussion and others (2019) as,

$$Z_b = Z_s - H \quad \textbf{(6)}$$

https://doi.org/10.1017/jog.2025.37 Published online by Cambridge University Press

where z_s is the ice surface elevation and H is the estimated ice thickness. We account for uncertainty in this term by recalculating z_b using $H \pm H_{err}$ as well, where H_{err} is the pixel-wise thickness uncertainty raster provided by Millan and others (2022). We computed the distance from the glacier terminus to the point where the glacier bed elevation first exceeds the current lake elevation (Z_L), at which point the lake-terminating glacier will become land-terminating. We estimated the elapsed time for each glacier to retreat to this point (t_{land}) based on the 1984 – 2021 mean rate as well as the more recent 2009 – 2018 rate. We assessed uncertainty in t_{land} by recalculating this timespan using upper- and lower-limit estimates of z_b provided by the H_{err} raster discussed above.

The height of the potentiometric surface above the glacier bed (d), equivalent to lake water depth once glacier retreat reaches that point, is estimated by subtracting the glacier bed elevation from the lake surface elevation (Z_L; Fig. 3), written

$$d = Z_L - Z_b \quad \textbf{(7)}$$

We then computed the median d value in the terminal 2 km (Fig. 3) to provide a single metric for comparing the flotation fraction to frontal ablation, retreat, and lake characteristics. We used a somewhat large 2 km length scale to assess conditions in the near-terminus environment to mitigate the impact of data quality issues, which are often most significant very close the terminus due to inappropriate boundary conditions (e.g., assuming ice thickness goes to zero; discussed in Recinos and others, 2019) or challenging environment for image correlation (e.g., very crevassed ice).

We ingested the semi-automated ice-marginal lake data from Rick and others (2022) to calculate the current area (averaged over 2016 – 2019; in this study we use 2018 as the effective lake area date) and area change (1984 – 2019) of each proglacial lake as well as its change over 1984 – 2018. Individual lake area and area change uncertainty is estimated as ± 1 pixel or ±30 m for Landsat imagery. We incorporate 2018 – 2022 accumulation area ratio data (i.e., the ratio between a glacier's accumulation area with its overall area) estimated from random forest classification of Sentinel 2 imagery from Zeller and others (accepted), available in the US Geological Survey's ScienceBase (https://dx.doi.org/10.5066/P1QHST6F). Lastly, we include 2010 – 2020 overall mass loss from Hugonnet and others (2021) derived from satellite geodesy. This mas loss dataset includes contributes from frontal ablation as well as surface mass balance.

https://doi.org/10.1017/jog.2025.37 Published online by Cambridge University Press

For all statistical analyses in this study, we used the non-parametric Kendall correlation test and Theil-Sen best fit line estimator. These statistical methods are resistant to outliers and do not assume data are distributed normally, which often makes them more suitable to analyzing "noisy" environmental datasets than traditional statistical methods such as Pearson correlation and ordinary least squares regression (Helsel and others, 2020).

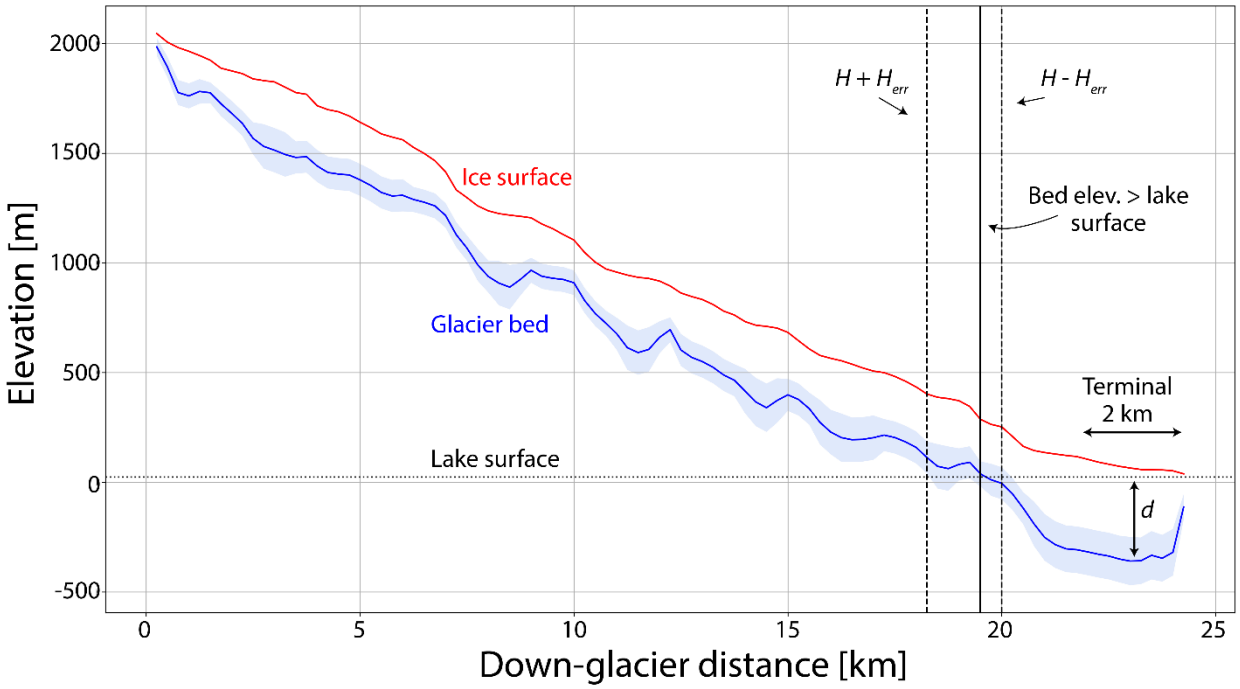

Figure 3. Surface (red) and bed elevation (blue) for Alsek Glacier (RGI60-01.23654). Uncertainty in bed elevation (blue fill; $\pm H_{err}$) is from the pixelwise thickness uncertainty raster provided by Millan and others (2022). The horizontal dotted line shows the lake surface elevation. The vertical lines show the point at which the glacier bed rises above the lake surface elevation using the estimated ice thickness (solid line) as well as the lower and high-end bounds of ice thickness (dashed lines). The median water depth in the terminal 2 km (d) is also illustrated.

https://doi.org/10.1017/jog.2025.37 Published online by Cambridge University Press

3. Results

3.1 Retreat rates of Alaska's lake-terminating glaciers

The annual terminus position time series show that 54 of the 55 lake-terminating glaciers retreated over 1984 – 2021 (Fig. 4). The only glacier to advance is Hole in The Wall Glacier near Juneau, AK (RGI60-01.27102), which advanced 263 m (5.8 m a^{-1}). Hole in the Wall Glacier is a distributary branch of Taku Glacier, whose multi-decadal tidewater advance diverging from regional average behavior is well-documented (McNeil and others, 2020). The median retreat over this period was 2.1 km (mean = 2.4 km), with the interquartile range spanning from 1.2 km to 3.1 km. The median retreat rate over the 1984 – 2018 period was 60 m a^{-1} (mean = 81 m a^{-1}) with the interquartile range spanning 35 – 89 m a^{-1} (Table S2). We note that the above retreat rates do not exactly correspond to the retreat distances because retreat rates are determined via a fit line while retreat distance is a simple difference between the first and last lengths. We use a 2018 end date here for consistency with lake area change data discussed in later analyses, as well as consistency with the input velocity datasets (Section 2.3). The fastest observed retreat rates (-751 m a^{-1} over 2009 - 2018) are found at East Yakutat Glacier (RGI60-01.12645), which retreated ~5.5 km since 2013 (750 m a^{-1}) when the east and west glacier branches separated. Several glaciers demonstrate non-monotonic retreat due to period re-advances due to surging (e.g., Bering Glacier; RGI60-01.13635; Fig. 4c orange line). Other glaciers (e.g., Grand Plateau – Alsek; RGI60-01.23655; Fig. 4d pink line) show stepped retreat, with large changes in terminus position between annual images, sometimes surrounded by periods of slower change.

The southeastern portion of the study area underwent more pronounced retreat, with RGI Region 01 sub-regions 05 and 06 (respectively St Elias Mountains and Northern Coast Ranges) retreating more on average than other locations (Figure 4). In particular, higher retreat rates (>100 m a^{-1}) are clustered in southeast Alaska's Fairweather Range and Juneau Icefield, with the rest of the study area featuring a mix of glaciers retreating slowly (0 – 50 m a^{-1}) or at intermediate rates (50 – 100 m a^{-1}) with no obvious spatial coherence for either the 2009 – 2018 period used for frontal ablation estimates (Fig. 5) or the full 1984 – 2021 study period (Fig. S6) retreat rates.

https://doi.org/10.1017/jog.2025.37 Published online by Cambridge University Press

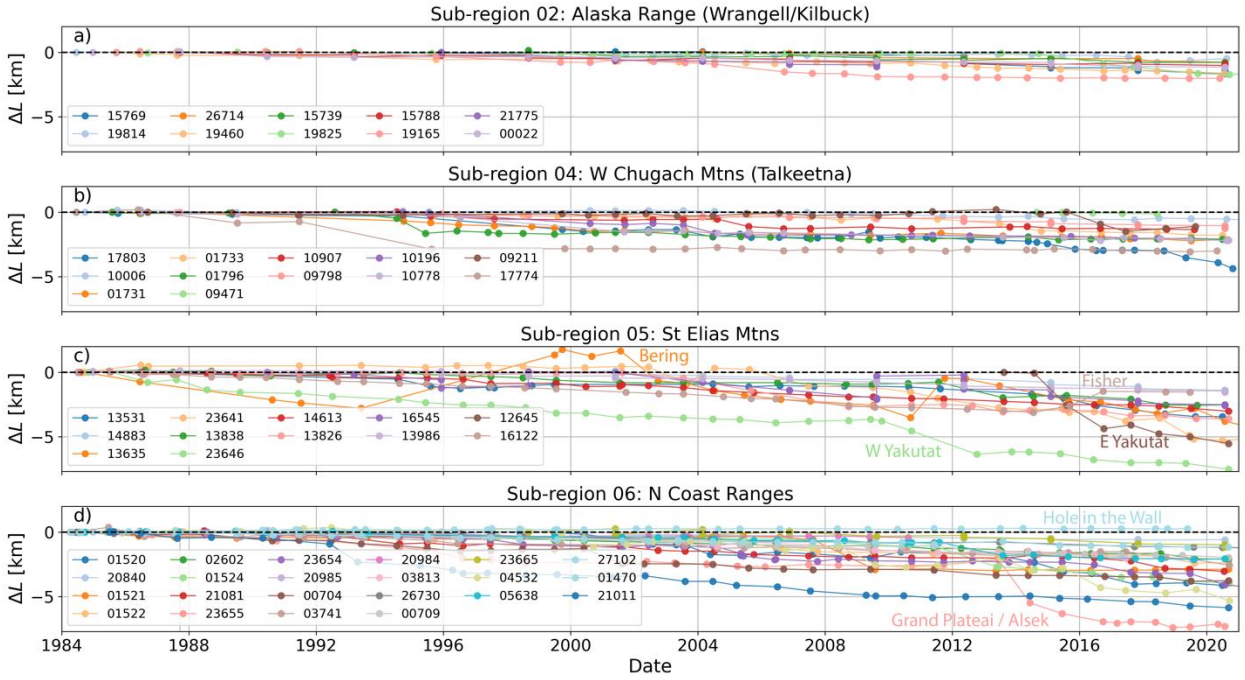

Figure 4. Length change (ΔL) time series for the 55 lake-terminating glaciers in this study, for a) RGI sub-region 01-02 (Alaska Range); b) sub-region 01-04 (W Chugach Mtns); c) sub-region 01-05 (St Elias Mtns); and d) sub-region 01-06 (N Coast Ranges).. Negative length change indicates retreat. The legend in the lower left of each panel contains the RGI IDs for each glacier, where the leading "RGI60-01." has been truncated.

https://doi.org/10.1017/jog.2025.37 Published online by Cambridge University Press

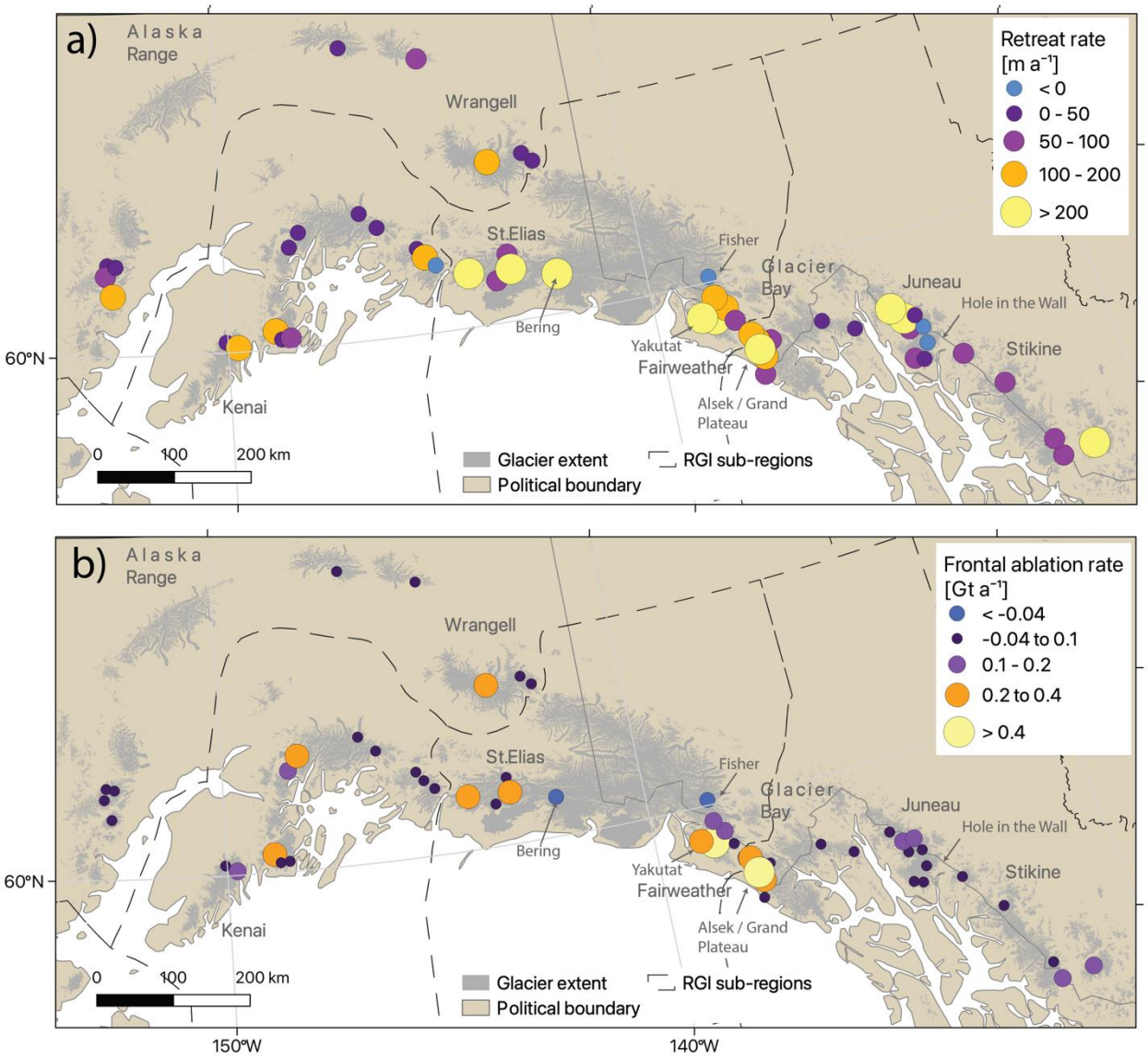

Figure 5. a) Spatial distribution of retreat rates (2009 – 2018) and b) frontal ablation rates on lake-terminating glaciers across RGI region 01. A version of this figure using full-record retreat rates to calculate frontal ablation is shown in Fig. S6. Map is projected in Alaska Albers (EPSG:3338).

3.2 Temporal variations in lake-terminating glacier retreat rates

The annual resolution of the glacier length time series allows investigation of changes in the rates of glacier retreat. On an individual glacier basis, we found widely-varying behavior. Of the 49 study glaciers that were lake-terminating throughout the entire 1984 – 2021 study period (i.e., excluding 6 glaciers that either developed or detached from their proglacial lake over the study period), 12 (24%) increased their rate of retreat across the three ~decadal periods, while the

https://doi.org/10.1017/jog.2025.37 Published online by Cambridge University Press

rate of retreat progressively slowed (or even changed to advance) for 4 (8%) glaciers (Fig. S7). For the remaining glaciers, 17 (35%) accelerated their retreat rate before slowing, while 16 (33%) slowed then accelerated their retreat rate.

Analyzing all 55 study glaciers together, the median retreat rate increased by 123% (30 to 67 m a^{-1}) from the 1986 – 1998 period to 2009 – 2018 (Figure 6; Table S2). The retreat value of every percentile became more negative (Table S2), indicating that the retreat rates of both the slowly and rapidly changing glaciers are accelerating. However, both metrics of regional inter-period retreat rate variability (interquartile range and span [5 – 95%]) increased over time, indicating a widening divide between the fastest and slowest retreating glaciers.

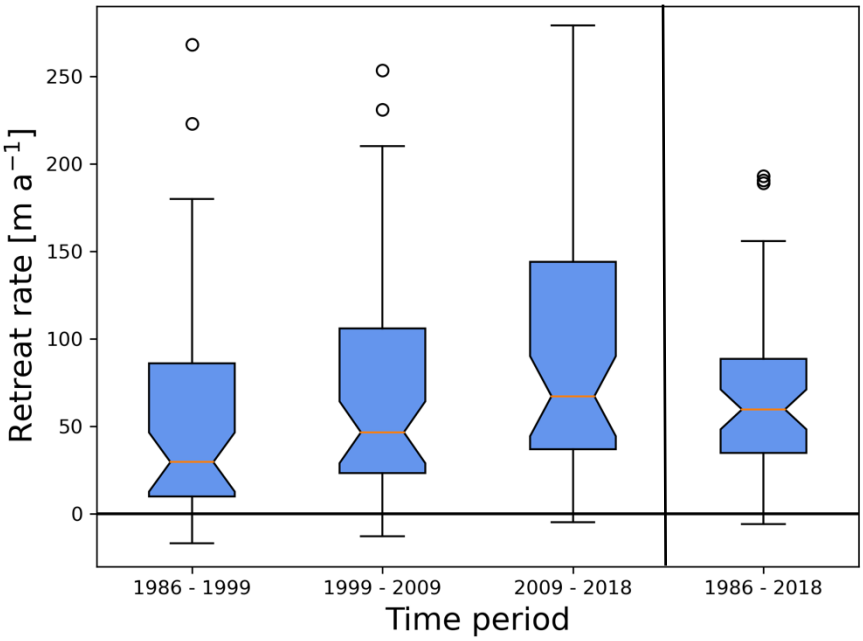

Figure 6. Box and whisker plots depicting retreat rates for the 55 study glaciers for the various periods, as well as the entire study period. The horizontal black line delineates retreat (rates > 0) from advance (rates < 0).

3.3 Estimates of frontal ablation

By combining our 2009 – 2018 average retreat rates and existing geospatial datasets for ice thickness and velocity, we estimated a median frontal ablation rate of 0.04 Gt a^{-1} (interquartile range (IQR) = 0.01 – 0.15) for the 55 lake-terminating study glaciers. Frontal ablation varies widely between different glaciers, with two glaciers losing ≥0.5 Gt a^{-1} to frontal

https://doi.org/10.1017/jog.2025.37 Published online by Cambridge University Press

ablation (East Yakutat Glacier, RGI60-01.12645; Grand Plateau – Alsek Glacier, RGI60-01.23655). Eight glaciers have frontal ablation rates between 0.2 – 0.5 Gt a^{-1} and nine have frontal ablation rates between 0.1 – 0.2 Gt a^{-1}. The majority of study glaciers (58%; n=32) have frontal ablation rates between –0.01 – 0.1 Gt a^{-1} (Figure S8). Negative values of F imply non-physical mass gain through ice accretion at the terminus, which we do not expect in this setting. Instead, negative F values reflect improper closure of the mass budget below the flux gate, due to uncertainties in the input datasets (Sec. 2.4), the assumed terminal surface mass balance (Sec. 2.3; Fig. S4), and/or temporal mismatch between input datasets. We thus take the small negative estimates described above to reflect essentially zero mass loss through frontal ablation. Two glaciers (Bering Glacier and Fisher Glacier; RGI60-01.16122) have substantially negative F estimates of –0.56 and –0.15 Gt a^{-1}. Both of these glaciers underwent surges in the early part of the 2009 – 2018 retreat rate period used for frontal ablation, but had reached quiescence by the 2017 – 2018 date (Burgess and others, 2012; Partington, 2023) described by the Millan and others (2022) surface velocities, resulting in low ice discharge (Q_{in}) estimates. For Fisher Glacier, Eqn 2 produces a negative frontal ablation (signifying ice accretion) to explain the glacier's advance, which is actually due to surge dynamics and should thus be ignored as a non-physical result. The piedmont geometry of Bering Glacier results in a very large surface areas below its flux gate, and our assumed high melt rate of $\dot{b}$ = –10 m a^{-1} results in a significant overestimate of surface melt, which produces a negative frontal ablation estimate because the calculated surface melt is greater than the incoming ice discharge. This error is exacerbated by the Q_{in} estimate being biased low due to the above-referenced timing mismatch between its recent surge and the velocity dataset. For Bering Glacier, we estimate 1.96 Gt a^{-1} loss to surface melt below the flux gate (Q_{melt}), and either reducing the Q_{melt} by 40% (corresponding to $\dot{b}$ = -7.1 m a^{-1}) or increasing Q_{in} seventeen-fold is required to produce the physically-expected F > 0 Gt a^{-1} for this glacier. In all likelihood, both terms are likely in error, as the glacier's terminal $\dot{b}$ was estimated to be close to -8 m a^{-1} over 1951 – 2011 (Tangborn, 2013) and a recent study showed the Millan and others (2022) ice thickness estimates (an input to Q_{in}) had high uncertainty for Sít' Tlein (Malaspina Glacier), a nearby glacier with similar piedmont morphology (Tober and others, 2023). Bering Glacier is an especially challenging case for the application of Equation 2 due to its surge history and large, unconstrained piedmont lobe, and we thus argue that a nonphysical F estimate at this one glacier does not invalidates the rest of the data we present

https://doi.org/10.1017/jog.2025.37 Published online by Cambridge University Press

here.

Summed across all study glaciers with positive *F* values, the collective rate of mass loss through frontal ablation is 6.1 Gt a^{-1} over 2009 – 2018. Using the slower 1984 – 2021 retreat rates results in a regional frontal ablation loss of 4.9 Gt a^{-1}, which sums to 183 Gt if the rate is held constant for the study period. Our study glaciers represent 83% of the region's lake-terminating glaciers as identified by the RGI v6 by area, but they are the largest or fastest retreating glaciers. We therefore suspect that the remaining 27% of RGI region 01 lake-terminating glacier area will increase regional frontal ablation loss by substantially less than 27%.

Varying frontal ablation rates are found throughout the region, with little evidence for large-scale spatial patterns (Fig. 5b). However, the Fairweather Range features a high density of glaciers with large frontal ablation rates (e.g., Yakutat, Grand Plateau, and Alsek glaciers). Additionally, the interior ranges (i.e., Alaska & Wrangell) do not host many glaciers with high frontal ablation rates (Fig. 5b).

3.4 Comparing lake- and marine-terminating glaciers

Comparing lake- and marine-terminating glaciers, we find differing patterns of retreat and overlapping frontal ablation distributions. McNabb and others (2015) found that only ~60% (16 of 27) of marine-terminating glaciers retreated over 1984–2013, while we show that nearly all (98%, 54 of 55) lake-terminating glaciers retreated over the same timespan (Fig. 7). On average, marine-terminating glaciers retreated approximately 20% slower than lake-terminating glaciers in this region, with a mean marine-terminating retreat rate of 47 m a^{-1} in comparison to the 58 m a^{-1} mean rate for lake-terminating glaciers. Comparing median rates, an even starker picture emerges, with marine-terminating glaciers retreating only 2 m a^{-1} on average, while the median lake-terminating glacier retreat rate was 51 m a^{-1}. The large discrepancy between mean and median retreat rates for marine-terminating glaciers is driven by the collapse of Columbia Glacier (RGI60-01.10689), which retreated 500 m a^{-1} on average over the study period.

https://doi.org/10.1017/jog.2025.37 Published online by Cambridge University Press

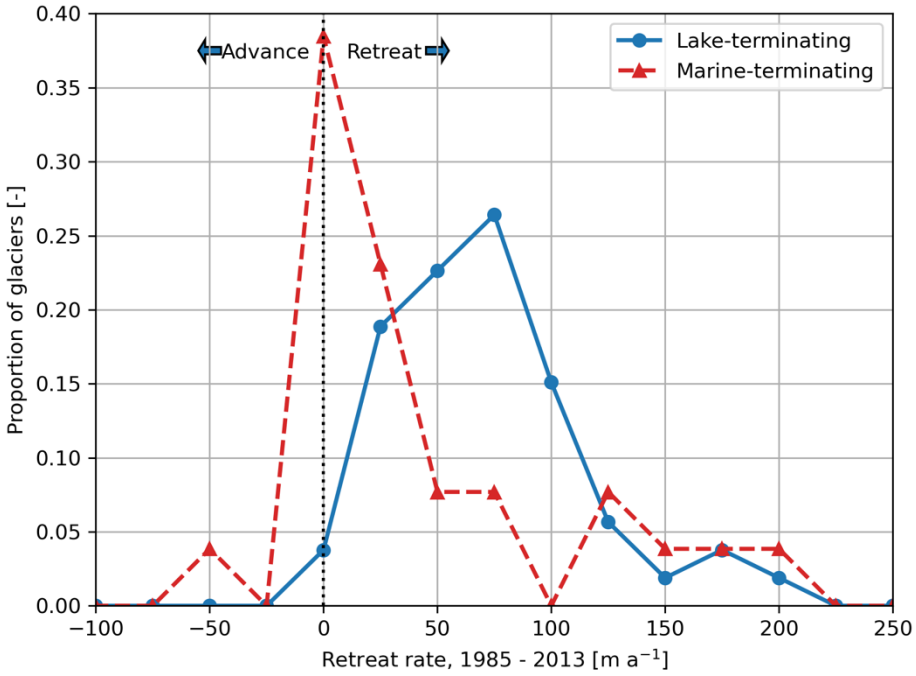

Figure 7. Histograms depicting the average retreat rate of lake-terminating (blue) and marine-terminating (red) glacier retreat from 1984 to 2013 (aligned with the McNabb and others (2015) marine-terminating dataset). Positive values indicate retreat while negative values represent advance. The marine-terminating Columbia Glacier retreat rate of 500 m a^{-1} is not shown for clarity.

Marine-terminating glaciers generally have higher rates of frontal ablation than lake-terminating glaciers, with the median frontal ablation rate for marine-terminating glaciers (0.27 Gt a^{-1}) an order of magnitude larger than the median lake-terminating rate (0.04 Gt a^{-1}). However, substantial overlap exists between the tails of each frontal ablation distribution, with the 75th percentile lake-terminating frontal ablation rate (0.15 Gt a^{-1}) exceeding the 25th percentile marine-terminating frontal ablation rate (0.10 Gt a^{-1}; Figure S8). Physically, this means that while frontal ablation rates are on average higher for marine-terminating glaciers, the lake-terminating glaciers with the highest frontal ablation rates (top quarter) lose more mass through the terminus than the marine-terminating glaciers with the lowest frontal ablation rates (bottom quarter). Comparing the slopes of the outlier-resistant Theil-Sen best fit lines, we find that a marine-terminating glacier on average loses 4.9 times more mass through frontal ablation than a lake-terminating glacier of equivalent area (Fig. 8a; marine-terminating slope = 10^{-3} Gt a^{-1} km^{-2}; lake-terminating slope = 2×10^{-4} Gt a^{-1} km^{-2}). However, lake-terminating glaciers retreat

https://doi.org/10.1017/jog.2025.37 Published online by Cambridge University Press

faster for a given frontal ablation rate (Fig. 8b).

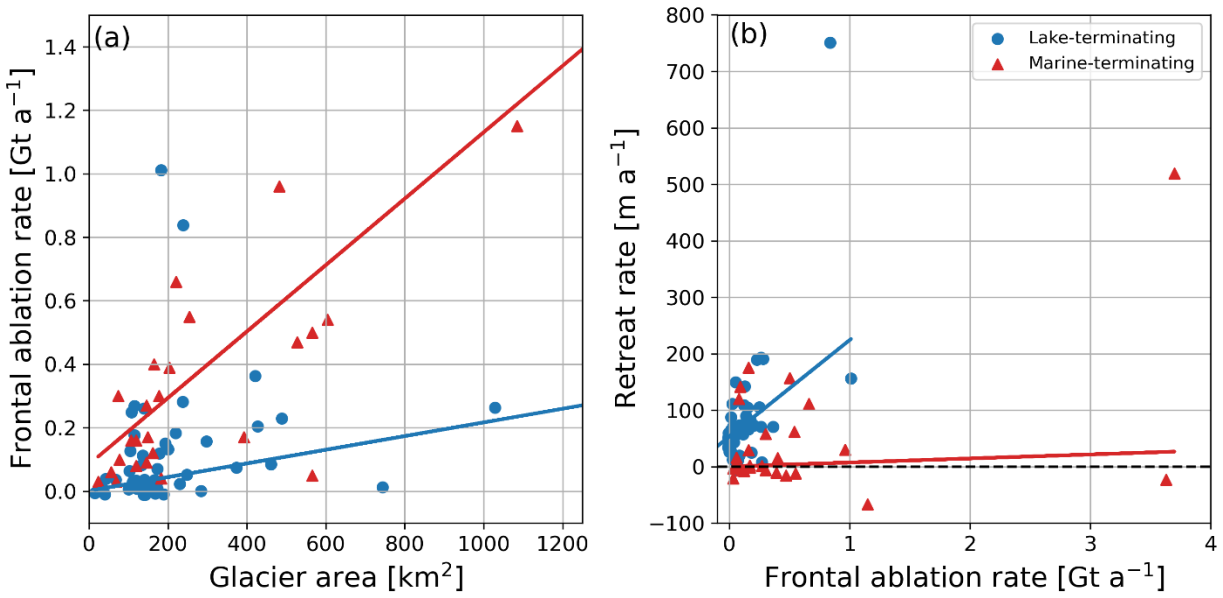

Figure 8. (a) Glacier area versus frontal ablation rate for lake-terminating (blue circles) and marine-terminating (red triangles) glaciers. **(b)** Study period average frontal ablation versus retreat rate for lake-terminating (blue) and marine-terminating (red) glaciers. Marine-terminating data is from McNabb and others (2015). Marine-terminating glaciers with outlying frontal ablation rates and/or areas (Columbia Glacier, F = 3.7 Gt a^{-1}, area = 944 km^2; Hubbard Glacier, F = 3.6 Gt a^{-1}, area = 3402 km^2) as well as lake-terminating glaciers with substantially negative F values (discussed in text; Bering Glacier, F = -0.56 Gt a^{-1}, area = 3025 km^2; Fisher Glaciers, F = -0.15 Gt a^{-1}, area = 441 km) are not shown for clarity.

3.5 Investigating potential physical drivers of lake-terminating retreat and frontal ablation

We find several associations between environmental variables and both retreat and frontal ablation rates. Across Alaska, proglacial lake area has increased by 85% (543 km^2 to 1006 km^2) since 1984 (Rick and others, 2022). In situ data show that water depth generally increases with lake area (Cook and Quincey, 2015), and we find that the predicted water depth (d) in the terminal 2 km for each glacier scales with the 2018 lake area (τ= 0.32, p < 0.01). Retreat and frontal ablation rates over 2009 – 2018 are positively associated with lake area (respectively τ= 0.23, p < 0.01; τ= 0.51, p < 0.01; Fig. 9a) and near-terminus water depth (respectively τ= 0.22, p = 0.02; τ= 0.40, p < 0.01; Fig. 9b). Physically, the latter association means that glaciers with deeper water near the terminus on average experience higher rates of frontal ablation than others. There also appears to be an association between the length of the terminal overeepening and frontal ablation rates (Fig. 9c), suggesting that the glaciers that are presently losing the

https://doi.org/10.1017/jog.2025.37 Published online by Cambridge University Press

most mass to frontal ablation also have the most to lose over the long term.

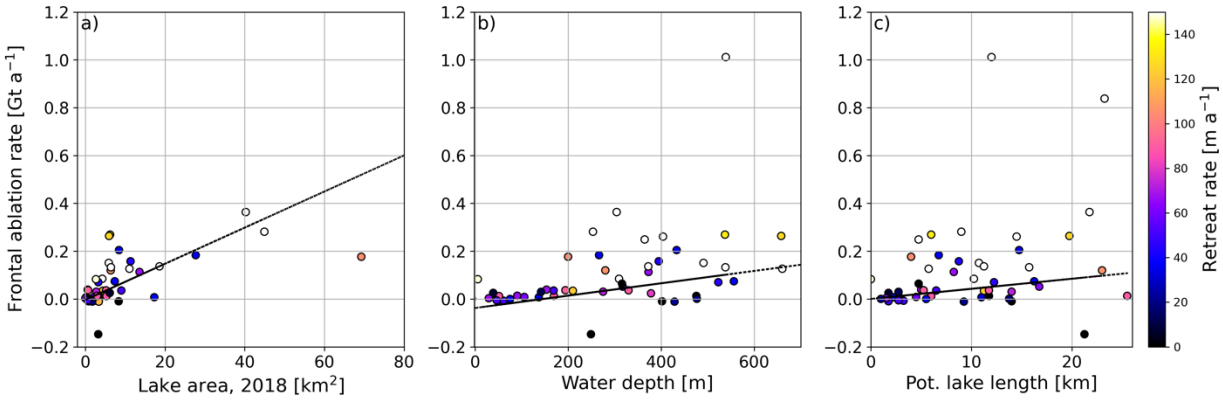

Figure 9. (a) Estimates of 2018 lake area versus frontal ablation rate for Alaska's lake-terminating glaciers over 2009 – 2018. Color bar indicates rate of glacier retreat, with warmer colors (e.g., yellow and white) indicating faster rates over 2009 – 2018. **(b)** Median potential lake depth versus rates of frontal ablation. **(c)** Length to the point where the glacier bed rises above the proglacial lake elevation, using the best guess ice thickness.

3.6 Projecting transition from lake- to land-terminating glaciers

When lake-terminating glaciers recede from their terminal overdeepenings, they transition to land-terminating and therefore lose frontal ablation as a mass loss term. To provide a first-order estimate for when these glaciers transition to a land-terminating state, we estimate the median distance from a lake-terminating glacier's terminus to the first point where the glacier bed rises above the lake surface elevation (at the time of the GLO-90 DEM, corresponding to 2011 – 2015). We find a median distance of 9.0 km to the end of the terminal overdeepening, though on a glacier-by-glacier basis, substantial variation exists in both terminal overdeepening lengths (IQR = 4.6 – 14 km; Fig. 10a) and retreat rates (IQR = 37 – 144 m a^{-1}), which yields a wide range in the projected time to transition to a land-terminating condition (t_{land}; IQR = 38 to 177 years; median = 74 years) based on 2009 – 2018 retreat rates (Fig. 10b). For some glaciers, it could be centuries before the glacier is land-terminating if they continue to retreat at their 2009 – 2018 rate, with the 90th percentile t_{land} being 279 years. The potential distance at which a glacier's bed rises above the lake surface elevation varies by 4.9 km (51%) on average due to uncertainty in ice thickness, with a larger range found for glaciers with larger glaciers with lower surface slopes. Using the low- and high-end estimates of ice thickness result in median t_{land} values ranging from 48 to 91 years using the 2009 – 2018 retreat rates. Using the slower

https://doi.org/10.1017/jog.2025.37 Published online by Cambridge University Press

retreat rates averaged over the full 1984 – 2021 study period gives a median t_{land} value of 118 years using the middle ice thickness estimate.

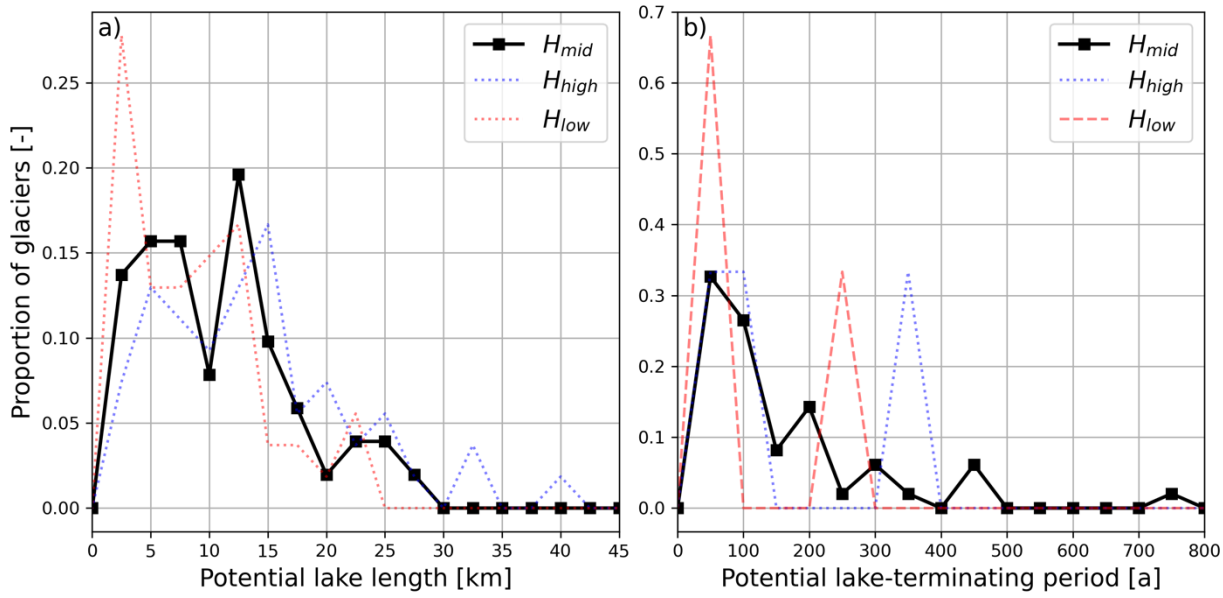

Figure 10. (a) Distribution of distance upstream from the terminus along centerline profiles to the point where the glacier bed elevation is above the current lake elevation using the Millan and others (2022) ice thickness distribution (black solid line) as well as upper- (blue dashed) and lower-end (red dashed) estimates based on the pixel-wise thickness uncertainty provided by that dataset. (b) Distribution of the time required for a glacier to reach these points if glacier retreat continues at the 2009 – 2018 rate. As in (a), line style reflects whether the middle, upper-, and lower-end ice thickness estimate from Millan and others (2022) is used in the calculation.

4. Discussion

Above, we estimated retreat and frontal ablation rates for Alaska and northwest Canada's lake-terminating glaciers, compared these values to the regions marine-terminating glaciers, investigated associations between these rates and lake characteristics, and estimated how long the glaciers will remain lake-terminating using existing geospatial datasets. Below, we interpret these results and put them in their scientific context. First, we delve deeper into the factors behind the region's widely varying lake-terminating frontal ablation rates and identify glaciers diverging from the regional norm. Later, we attempt to reconcile the region's disparate lake- and marine-terminating glaciers thinning rates given our results and the area's glacier history. Finally, we look forward using the example of Patagonia and our estimates for the duration over which our study glaciers will remain in contact with their proglacial lakes to envisage the future of Alaska's lake-terminating glaciers.

https://doi.org/10.1017/jog.2025.37 Published online by Cambridge University Press

4.1 Parsing contributions to frontal ablation

To develop a greater understanding of what sets the rate of frontal ablation across our lake-terminating study glaciers, we dissect Eqns 1 and 2 to investigate the absolute and relative contributions to *F* of ice flux through the flux gate (Q_{in}), terminus retreat $A\frac{dL}{dt}$ (Q_{ret}), and surface melt in the region between the flux gate and terminus ($Q_{melt} = \dot{b}S$). This analysis allows discrimination of cases in which a high frontal ablation rate is produced from the disintegration of a slow-moving tongue ($Q_{ret} \gg Q_{in}$) from cases of glaciers that are closer to steady state ($Q_{ret} \approx 0$) despite high mass loss through frontal ablation ($Q_{in} \gg Q_{ret}$). We interpret a high ratio of Q_{in}/Q_{ret} (i.e., >>1) to reflect "active" frontal ablation where the high ice discharge may allow the upstream glacier to respond more sensitively to terminus conditions via positive feedbacks between frontal ablation and glacier geometry. By contrast, a large *F* can also be obtained by a high Q_{ret} and low Q_{in} ($\frac{Q_{in}}{A\frac{dL}{dt}} \ll 1$), which we consider "passive" frontal ablation because it is driven more by a lack of Q_{in} across the flux gate (the integral of upstream surface mass balance) rather than anything occurring at the glacier terminus. In most cases, we find terminus retreat and incoming ice discharge contribute approximately equally to our *F* estimates (Fig. 11a 1:1 line), suggesting active processes at the glacier terminus and as well as glacier-wide processes share responsibility for frontal ablation on the majority of study glaciers. However, several outliers from this relationship exist, suggesting that these glaciers are undergoing substantially different frontal ablation processes than the regional norm. Prominent examples where terminus retreat dominates *F* are Bering Glacier (RGI60-01.13635) and East Yakutat Glacier (RGI60-01.12645). As discussed in Sec. 3.3, Bering Glacier underwent a surge during 2008 – 2011 (Burgess and others, 2012), resulting in an "overextended" terminus that subsequently retreated and slow surface velocities during the 2009 – 2018 period for *F* estimations. East Yakutat Glacier had a floating tongue that began to disintegrate in 2010 (Trüssel and others, 2013). The glacier drains the low-elevation Yakutat Icefield, whose highest reaches are at times below the end-of-summer snowline, leaving the glacier with little to no accumulation zone (Trüssel and others, 2013). In both of these cases, the glaciers have insufficient accumulation area to provide the high mass flux required to balance melt in their extensive low lying regions, and would thus undergo substantial retreat even in the absence of calving and subaqueous melt. Indeed, Trüssel and others (2015) found that

https://doi.org/10.1017/jog.2025.37 Published online by Cambridge University Press

incorporating a frontal ablation parameterization had little effect on the evolution of Yakutat Glacier, with its 21st century evolution driven largely by surface mass balance.

In most cases surface melt below the flux gate is substantially smaller than the incoming ice flux (blue points on Fig. 11a, red dots on Fig. 11b), even with the conservatively assumed terminal surface mass balance rate $\dot{b}$ = –10 m a^{-1}. However, there are cases where $Q_{melt} > Q_{in}$ (blue points on Fig. 11b). These cases could result from our assumed melt rate being too high or modeled ice thickness too low, which will produce unrealistically low frontal ablation rates. However, these cases could also be explained by glacier retreat on these glaciers being dominated by declining surface mass balance over the whole glacier, such that the incoming ice discharge (Q_{in}; which integrates the upstream surface mass balance) in insufficient to balance melt in the terminal region. If the second explanation were true, these glaciers would essentially act like land-terminating glaciers, with frontal ablation playing a limited role in their ongoing retreat.

https://doi.org/10.1017/jog.2025.37 Published online by Cambridge University Press

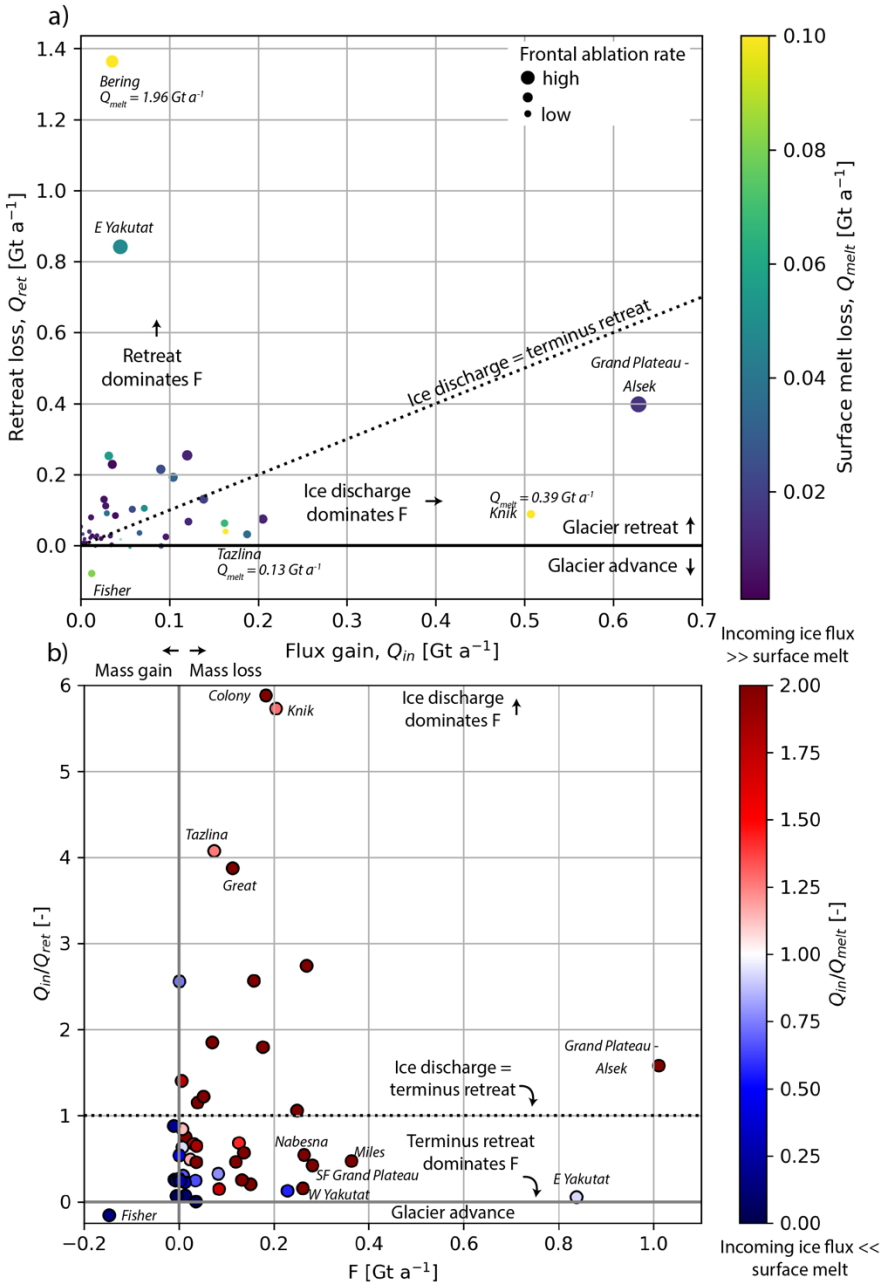

Figure 11. Parsing the contribution of frontal ablation in terms of the a) absolute and b) relative values of terms in Eqn 2. In a), points are scaled by the estimated frontal ablation rate (F) and colored by the mass loss to surface melt in the region below the flux gate (Q_{melt}). In b), the y-coordinate of each point reflects the balance of ice discharge Q_{in} and terminus retreat (Q_{ret}) at setting the frontal ablation rate. A value of 1 on this axis indicates Q_{in} and Q_{ret} contribute equally to F, where values >> 1 and 0 respectively indicate dominance of Q_{in} or Q_{ret} in setting F. The color axis in b) shows the proportion of Q_{in} is expected to be lost to surface melt between the flux gate and terminus. The signs of Q_{ret} and Q_{melt} are inverted for clarity on this plot, but they are in fact negative in almost all cases, as shown in Equation 1. On both panels, the names of outlying glaciers are given in gray text. In b), Bering Glacier is omitted due to its substantially negative F estimate, discussed in Sec. 3.3.

https://doi.org/10.1017/jog.2025.37 Published online by Cambridge University Press

4.2 Contextualizing differences between lake- and marine-terminating glaciers

In other studies, lake-terminating glaciers are associated with higher rates of mass loss than land-terminating glaciers (King and others, 2019; Maurer and others, 2019) as well as marine-terminating glaciers (Larsen and others, 2015). During the 2000-2015 time-period, King and others (2019) found that lake-terminating glaciers in the Himalaya experienced nearly 1.5 times more negative mass balance than land-terminating glaciers, and that this discrepancy had increased over time. While substantial differences exist between Himalayan and Alaskan glaciers, and covariance between terminus type and other attributes may exist (e.g., elevation, ice thickness) this study suggests mass loss enhancement in glaciers terminating in lakes. The Larsen and others (2015) study used airborne altimetry to show that lake-terminating glaciers contribute 4 times as much to total Alaskan glacier mass loss than marine terminating (6% vs 24%). Many of these studies suggest frontal ablation as a causative mechanism to explain differences in mass loss rates between terminus classes, but systematic analyses of the mass lost through frontal ablation in lake-terminating systems remain sparse (Minowa and others, 2021). Our dataset allows a direct estimate of the equivalent thinning frontal ablation on study glaciers would produce if the mass loss were spread uniformly across a glacier's entire surface area. The median equivalent thinning due to frontal ablation values is 0.25 m w.e. a^{-1} (interquartile range = 0.06 – 0.70 m w.e. a^{-1}) for our study glaciers. Converting the 2010 – 2020 total mass loss data from Hugonnet and others (2021; which includes the effects of both surface melt and frontal ablation) to average thinning rates (dividing volume loss by surface area), we find a median overall thinning rate for our lake-terminating study glaciers of 1.21 m w.e. a^{-1} (interquartile range = 0.94 – 1.55 m w.e. a^{-1}). We do not compute percentages of total loss due to frontal ablation because our frontal ablation estimates do not necessarily reflect a mass imbalance – a glacier in steady state could still have high mass loss through the terminus. However, comparing the relative magnitude of the mass loss terms, we show that mass loss from frontal ablation could be an important process in shaping the future evolution of the region's lake-terminating glaciers.

Considering the regional sum of positive F vales (6.1 Gt a^{-1}), we compute an area-weighted equivalent thinning rate of 0.62 m w.e. a^{-1} by dividing the F sum by the surface area of glaciers with positive F values (9700 km^2; notably, notably excluding Bering Glacier, the

https://doi.org/10.1017/jog.2025.37 Published online by Cambridge University Press

largest glacier in the dataset). This value is 45% of Alaska's area-weighted equivalent thinning rate for marine-terminating glaciers (1.37 m w.e. a^{-1}; McNabb and others, 2015).

Comparing median retreat rates, Alaska's lake-terminating glaciers retreated substantially faster than their marine-terminating counterparts (Fig. 7; 51 m a^{-1} vs 2 m a^{-1}) over 1984 – 2013 despite lake-terminating glaciers losing ~five times less mass through frontal ablation than a marine-terminating glacier of the same surface area. By investigating total mass loss over 2010 – 2010 (Hugonnet and others, 2021), we find that, while lake-terminating glaciers lose less mass to frontal ablation than marine-terminating glaciers, they are losing more mass overall. Lake-terminating study glaciers have a median total mass loss of 0.19 Gt a^{-1} (interquartile range = 0.11 – 0.36 Gt a^{-1}) compared with 0.08 Gt a^{-1} (0.03 – 0.29 Gt a^{-1}) for marine-terminating study glaciers.

Systematic differences between the lake- and marine-terminating glacier-wide mass balance due to differences in the hypsometry and accumulation area ratio could partly explain the apparent variation in retreat sensitivity to frontal ablation rates. Many of Alaska's marine-terminating glaciers underwent catastrophic tidewater retreat in the 19th and 20th centuries, prior to our study period, resulting in relatively stable states with high accumulation area ratios in the late 20th century (Larsen and others, 2015). Many of the current lake-terminating glaciers were land-terminating (or terminating in small and likely shallow lakes) during the same time period and may thus have responded more slowly to climate change because they lacked the additional mass loss term of frontal ablation, resulting in the glaciers being "overextended" relative to the modern climate with low accumulation area ratios. Indeed, the median accumulation area ratio (AAR) for our lake-terminating study glaciers is 0.46 (interquartile range = 0.34 – 0.52) compared with 0.59 (0.49 – 0 .73) for marine-terminating study glaciers, and this effect persists when dividing glaciers into their RGI sub-regions to account for potential climatic differences between lake- and marine-terminating glaciers (Figure 12). These findings are similar to those of Patagonia, where lake-terminating glaciers were found to have systematically lower accumulation area ratios (0.63 vs 0.85) and flatter ablation zones than their marine-terminating counterparts (Minowa and others, 2021). Thus, our comparison of lake- and marine-terminating glaciers may in some ways not reflect a difference in process, but a difference in their phase in the "tidewater glacier cycle" (Post, 2011) and resultant larger relative ablation areas that make lake-terminating glaciers respond

https://doi.org/10.1017/jog.2025.37 Published online by Cambridge University Press

more sensitively to modern climate warming. Indeed, in sub-region 06 (Northern Coast Ranges) where AAR distributions are similar between lake- and marine-terminating glaciers (Figure 12), median retreat rates between terminus classes are much more closer than for the entire Alaska region (46 m a^{-1} retreat for marine-terminating glaciers vs 66 m a^{-1} for lake-terminating glaciers over 1985 – 2013, respectively compared with 2 m a^{-1} and 51 m a^{-1} for the entire region).

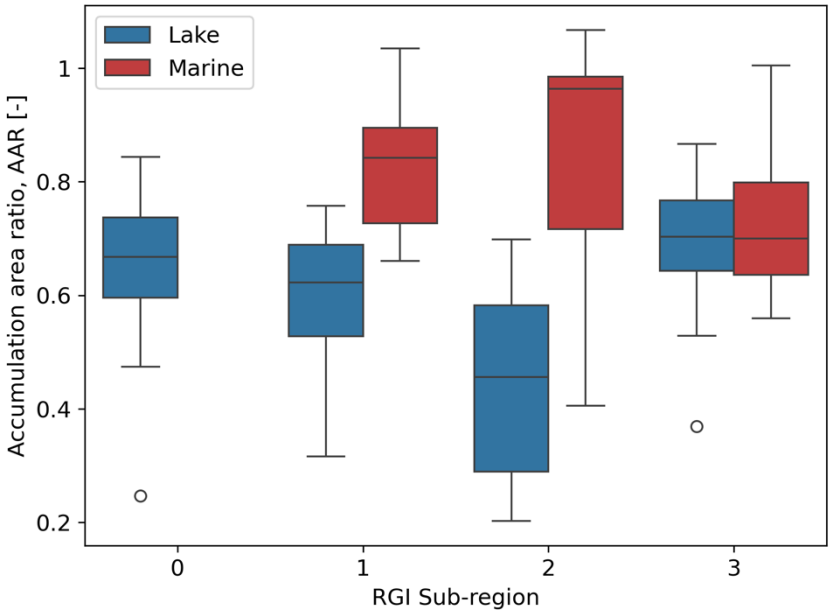

Figure 12. Summary of accumulation area ratio differences between lake- (blue) and marine-terminating (red) study glaciers. Glaciers are divided into RGI sub-regions (Figure 1) to control for climate regime. Sub-regions are defined as follows: 02 = Alaska Range, 04 = Western Chugach, 05 = St Elias; 06 = Northern Coast Ranges.

Nevertheless, our findings show that frontal ablation rates on lake-terminating glaciers can be comparable to those seen on marine-terminating glaciers. Frontal ablation may therefore be an important mass loss term for lake-terminating glaciers despite the presence of relatively cold water and the absence of a turbulent buoyant plume melt in the lakes (Benn and others, 2007a; Truffer and Motyka, 2016). The proliferation of proglacial lakes across Alaska coincides with accelerated thinning of Alaska glaciers (0.65 m a^{-1} over 2000 – 2004 to 1.24 m a^{-1} over 2015 – 2019; Hugonnet and others, 2021) and retreat rates of lake-terminating glaciers. This correspondence has led some authors (e.g., King and others, 2019) to postulate that the lakes themselves are causing the enhanced mass loss, but systematic differences in quantities such as ice thickness, accumulation area ratio, and elevation between terminus classes (e.g.,

https://doi.org/10.1017/jog.2025.37 Published online by Cambridge University Press

Yang and others, 2022) can confound such analyses. Estimates of mass loss through frontal ablation in freshwater systems over large spatial scales have only recently becoming available, with ~7 Gt a^{-1} lost through lacustrine termini in Patagonia (Minowa and others, 2021). In the Himalayas, recent work found that traditional geodetic estimates underpredicted mass loss by ~7% because they did not account for subaqueous mass loss (Zhang and others, 2023), but this study is based upon uncertain lake area-volume scaling. Together with these previous studies, our estimates of lake-terminating frontal ablation rates suggest that frontal ablation in Alaska currently is an important mass loss process for some lake-terminating glaciers.

4.3 Future Evolution of Alaska's Lake-Terminating Glaciers: Analog in Patagonia?

Alaska's ice-marginal lakes grew rapidly over the past 40 years (increasing in area by 85% between 1984 – 2019 to now cover 1000 km^2). and there is no sign of this trend slowing (Rick and others, 2022). Using the modern lake surface elevation, ice thickness estimates, and observed rates of glacier retreat, our data suggest that Alaska's lake-terminating glaciers will not retreat from their terminal overdeepenings and become land-terminating for many decades (median = 74 a; IQR = 38 – 177 a) if the glaciers continue to retreat at their 2009 – 2018 retreat rates.

Given our findings, the growth of proglacial lakes may have important consequences for the evolution of the region's lake-terminating glaciers. Larger lakes tend to be deeper (Cook and Quincey, 2015; Zhang and others, 2023). We find that frontal ablation rates tend to increasee with proglacial lake area and water depth (Figs. 9a-b), suggesting that lake-terminating glacier mass loss through frontal ablation will only increase as proglacial lakes grow and deepen. Glaciers could transition to a land-terminating condition earlier than projected above if future retreat rates are faster than those observed over the past decades.

While factors such as wind-driven overturn circulation strength and changes in water fluxes are likely important, it is plausible to imagine that as proglacial lake area increases, more surface area is available to absorb solar radiation, potentially warming surface waters and enhancing rates of subaqueous melt (Trüssel and others, 2015). Sparse in-situ observations in Alaska proglacial lakes show surface water temperatures < 3 °C (Boyce and others, 2007), yet observations on the larger proglacial lakes of Patagonia show water surface temperatures as high as 8 °C (Sugiyama and others, 2016). Further, ASTER remote sensing data in other parts of the

https://doi.org/10.1017/jog.2025.37 Published online by Cambridge University Press

world suggest that proglacial lakes could be warmer than the often-assumed uniform low (~1 °C) temperature (Dye and others, 2021). Thus, if Alaska's proglacial lakes warm towards Patagonian levels as they continue to grow, increased frontal ablation rates through enhanced subaqueous melt are possible.

In Patagonia, the average (meaning median) lake-terminating glacier lost 0.08 Gt a^{-1} (IQR = 0.02 – 0.25 Gt a^{-1}) through frontal ablation over 2000 – 2019 (Minowa and others, 2021), roughly double the rates we document in Alaska (median = 0.04 Gt a^{-1}; IQR = 0.01 – 0.15 Gt a^{-1}) over 2009 – 2018. In Patagonia, there is some evidence that frontal ablation rates increase superlinearly with increasing glacier area (best-fitting power-law area exponent = 1.2; Figure 13 thick orange line) while Alaska's lake-terminating frontal ablation rates increase sublinearly (area exponent = 0.46). If instead a linear fit is applied to the data, we find the slope of the best-fit line to Patagonia data is 3 times steeper than that for Alaska (Figure 13 thin lines). The explained variance (R^2) is substantially higher for the power-law fits in both cases (0.60 vs 0.42 for Patagonia; 0.07 vs -0.10 for Alaska), suggesting nonlinear relationships between glacier area and frontal ablation in both regions. Regardless of the functional form of the fit line, we find substantial overlap between Alaska and Patagonia frontal ablation rates for glaciers < 500 km^2, with the most pronounced difference seen for the regions' largest glaciers (Fig. 13). The termini of many Patagonia glaciers are steep and fast flowing due to regional topography (Minowa and others, 2023), which could partly explain the differences in frontal ablation rates. However, the Patagonia glaciers with the highest frontal ablation rates terminate in lakes orders of magnitude larger than the Alaska glaciers (Fig. 13), which could have a substantial effect as well. As Alaska's lake-terminating glaciers continue to retreat, they move into more confined valleys, which could promote steepening and faster terminus velocities. This dynamic, in addition to their growing (and perhaps warming) proglacial lakes, could mean that Alaska's future lake-terminating glaciers look much more similar to the Patagonian example than they do at present.

https://doi.org/10.1017/jog.2025.37 Published online by Cambridge University Press

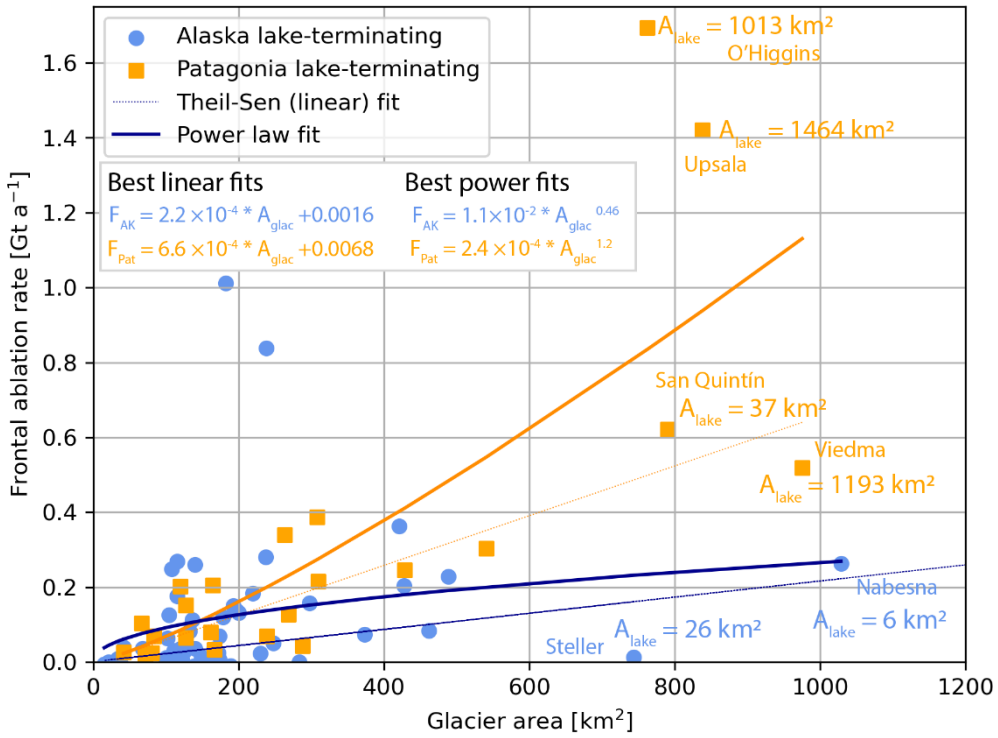

Figure 13. Comparison of frontal ablation rates between Alaska (blue circles) and Patagonia (orange squares) lake-terminating glaciers as a function of glacier area. Equations for the Sen slope linear best fit to data from each region are displayed in the upper left, where the units of frontal ablation and glacier area (A_{glac}) are respectively Gt a^{-1} and km^2. Lake area for large glaciers are indicated in colored text. Data from Patagonia are reported in Minowa and others (2021).

5. Conclusions

The role of proglacial lakes in glacier change is receiving more attention as proglacial lakes proliferate and grow around the world, yet estimates of additional mass loss due to these lakes are sparse. We investigate Alaska and northwestern Canada, a region with rapid proglacial lake expansion, and find that lake-terminating glaciers retreated a median rate of 60 m a^{-1} (IQR = 35 – 89 m a^{-1}) over 1984 – 2018 and lost 0.04 Gt a^{-1} (IQR = 0.01 – 0.15 Gt a^{-1}) of ice through frontal ablation over 2009 – 2018. While the data we report here do not necessarily reflect an imbalance, mass loss through frontal ablation is significant when compared the 2010 – 2020 median total mass loss rate of 0.19 Gt a^{-1} for our study glaciers. The region's lake-terminating glaciers retreated substantially faster than its marine-terminating glaciers, despite lake-terminating glaciers losing five times less mass through frontal ablation than marine-terminating glaciers of equivalent area (Figure 8). The difference in retreat rates may be due to lake-

https://doi.org/10.1017/jog.2025.37 Published online by Cambridge University Press

terminating glaciers showing systematically lower accumulation area ratios than the region's marine-terminating glaciers (0.46 vs 0.59), which indicates they are more out of balance with the current climate. We compare our results with existing geospatial datasets and find positive relationships between frontal ablation and lake area and terminal water depth. Large lakes are associated with greater water depth, frontal ablation, and retreat rates. As the region's proglacial lakes continue to expand, they may warm and/or deepen, only increasing rates of mass loss though frontal ablation to become more similar to Patagonian glaciers. We find that most of the region's lake-terminating glaciers will likely remain so for at least the remainder of this century, making enhanced understanding of frontal ablation critical for projecting the long-term evolution of Alaska's lake-terminating glaciers. Our work provides a first-order estimate of losses to freshwater frontal ablation from remotely-sensed datasets and shows that this has been an important mass loss process for many lake-terminating glaciers in the past and could continue to play an important role in the evolution of the region's lake-terminating glaciers throughout the 21st century. The substantial mass lost through frontal ablation motivates its incorporation into models of glacier changes. Parameterizations of freshwater frontal ablation must differ from those applied in marine-terminating environments and should be based on detailed in situ observations such as proglacial lake bathymetry and hydrographic structure as well as subglacial topography. Constraining how lake-terminating frontal ablation processes operate at present and how they are likely to change in a warming climate could alter projections of glacier evolution with implications for management of future sea level rise, downstream water resources, and aquatic ecosystems.

Acknowledgements

This work was enabled by the data sharing and software development of many cryosphere community members (McNabb and others, 2015; RGI Consortium, 2017; Lea, 2018; Gardner and others, 2019; Millan and others, 2022). We gratefully acknowledge support from NSF-OPP-1821002, NSF-OPP-2334775, the Appalachian State University Honors College, and the Office of Student Research. Regine Hock aided in the interpretation of negative frontal ablation rates and provided suggestions on data presentation to improve the utility of our dataset for the global glacier modeling community. The detailed and constructive reviews provided by Scientific Editor Marius Schaefer, Will Kochtitzky, and one anonymous reviewer substantially improved

the quality of this manuscript.

Data and code availability

All data produced in the course of this work will be posted on Arctic Data Center by the time of manuscript publication and linked here. All code will be posted on Zenodo by the time of manuscript publication and linked here.

Ice thickness and velocity data are available from Millan and others (2022; https://doi.org/10.6096/1007). Overall glacier mass change is from Hugonnet and others (2021; https://doi.org/10.6096/13). Proglacial lake area data are from Rick and others (2022; https://doi.org/10.18739/A2MK6591G). Surface elevation data are from the Copernicus GLO90 digital elevation model (https://doi.org/10.5270/ESA-c5d3d65). Accumulation area ratios are provided by Zeller and others (accepted; https://dx.doi.org/10.5066/P1QHST6F). The Randolph Glacier Inventory is available at https://doi.org/10.5067/f6jmovy5navz.

Author Contributions

NC completed primary data generation, post processing, data analysis, drafting original manuscript text and text revision. WA secured funding, conceived project idea, performed geospatial data extraction, advised research direction, contributed to & edited the manuscript, and performed the bulk of the peer-reiew revisions. RM developed the dataset of frontal ablation for marine-terminating glaciers, provided discussion & feedback, and contributed to & edited the manuscript. EE provided discussion & feedback, and contributed to & edited the manuscript. DM supervised the development of the proglacial lake extent dataset, provided discussion & feedback, and contributed to & edited the manuscript. BR developed the dataset of proglacial lake extents, and provided discussion & feedback. JH developed a preliminary version of retreat time-series for lake-terminating glaciers. LBP provided discussion & feedback and edited the original manuscript.

https://doi.org/10.1017/jog.2025.37 Published online by Cambridge University Press

References

Benn DI, Warren CR and Mottram RH (2007a) Calving processes and the dynamics of calving glaciers. *Earth-Science Reviews* **82**(3–4), 143–179. doi:10.1016/j.earscirev.2007.02.002

Benn DI, Hulton NRJ and Mottram RH (2007b) 'Calving laws', 'sliding laws' and the stability of tidewater glaciers. *Annals of Glaciology* **46**, 123–130. doi:10.3189/172756407782871161

Boyce ES, Motyka RJ and Truffer M (2007) Flotation and retreat of a lake-calving terminus, Mendenhall Glacier, southeast Alaska, USA. *Journal of Glaciology* **53**(181), 211–224. doi:10.3189/172756507782202928

Brown CS, Meier MF and Post A (1982) Calving speed of Alaska tidewater glaciers, with application to Columbia Glacier. *Professional Paper*. doi:10.3133/pp1258C

Burgess EW, Forster RR, Larsen CF and Braun M (2012) Surge dynamics on Bering Glacier, Alaska, in 2008–2011. *The Cryosphere* **6**(6), 1251–1262. doi:10.5194/tc-6-1251-2012

Carrivick JL and 7 others (2022) Coincident evolution of glaciers and ice-marginal proglacial lakes across the Southern Alps, New Zealand: Past, present and future. *Global and Planetary Change* **211**, 103792. doi:10.1016/j.gloplacha.2022.103792

Carrivick JL and Tweed FS (2013) Proglacial lakes: character, behaviour and geological importance. *Quaternary Science Reviews* **78**, 34–52. doi:10.1016/j.quascirev.2013.07.028

Chen F and 6 others (2021) Annual 30 m dataset for glacial lakes in High Mountain Asia from 2008 to 2017. *Earth System Science Data* **13**(2), 741–766. doi:10.5194/essd-13-741-2021

Cook SJ and Quincey DJ (2015) Estimating the volume of Alpine glacial lakes. doi:10.5194/esurfd-3-909-2015

Cuffey KM and Paterson WSB (2010) *The physics of glaciers.*, Fourth edition. Elsevier, San Diego.

Dorava JM and Milner AM (2000) Role of lake regulation on glacier-fed rivers in enhancing salmon productivity: the Cook Inlet watershed, south-central Alaska, USA. *Hydrological Processes* **14**(16–17), 3149–3159. doi:10.1002/1099-1085(200011/12)14:16/17<3149::AID-HYP139>3.0.CO;2-Y

Dye A, Bryant R, Dodd E, Falcini F and Rippin DM (2021) Warm Arctic Proglacial Lakes in the ASTER Surface Temperature Product. *Remote Sensing* **13**(15), 2987. doi:10.3390/rs13152987

European Space Agency (2024). *CopernicusGlobal Digital Elevation Model*. Distributed by OpenTopography. https://doi.org/10.5069/G9028PQB Accessed: 01 May 2023

Farinotti D, Round V, Huss M, Compagno L and Zekollari H (2019) Large hydropower and water-storage potential in future glacier-free basins. *Nature* **575**(7782), 341–344. doi:10.1038/s41586-019-1740-z

Gardner A, Fahnestock M and Scambos T (2022) MEaSUREs ITS_LIVE Regional Glacier and Ice Sheet Surface Velocities, Version 1. doi:10.5067/6II6VW8LLWJ7

Helsel DR, Hirsch RM, Ryberg KR, Archfield SA and Gilroy EJ (2020) Statistical methods in water resources. 4-A3. U.S. Geological Survey. doi:10.3133/tm4A3

How P and 10 others (2021) Greenland-wide inventory of ice marginal lakes using a multi-method approach. *Scientific Reports* **11**(1), 4481. doi:10.1038/s41598-021-83509-1

Hugonnet R and 10 others (2021) Accelerated global glacier mass loss in the early twenty-first century. *Nature* **592**(7856), 726–731. doi:10.1038/s41586-021-03436-z

King O, Bhattacharya A, Bhambri R and Bolch T (2019) Glacial lakes exacerbate Himalayan glacier mass loss. *Scientific Reports* **9**(1), 18145. doi:10.1038/s41598-019-53733-x

Kochtitzky W and 17 others (2022) The unquantified mass loss of Northern Hemisphere marine-terminating glaciers from 2000–2020. *Nature Communications* **13**(1), 5835. doi:10.1038/s41467-022-33231-x

Larsen CF, Burgess E, Arendt AA, O'Neel S, Johnson AJ and Kienholz C (2015) Surface melt dominates Alaska glacier mass balance. *Geophysical Research Letters* **42**(14), 5902–5908. doi:10.1002/2015GL064349

Lea JM (2018) The Google Earth Engine Digitisation Tool (GEEDiT) and the Margin change Quantification Tool (MaQiT) – simple tools for the rapid mapping and quantification of changing Earth surface margins. *Earth Surface Dynamics* **6**(3), 551–561. doi:10.5194/esurf-6-551-2018

Main B and 11 others (2023) Terminus change of Kaskawulsh Glacier, Yukon, under a warming climate: retreat, thinning, slowdown and modified proglacial lake geometry. *Journal of Glaciology* **69**(276), 936–952. doi:10.1017/jog.2022.114

Maurer JM, Schaefer JM, Rupper S and Corley A (2019) Acceleration of ice loss across the Himalayas over the past 40 years. *Science Advances* **5**(6), eaav7266. doi:10.1126/sciadv.aav7266

Maussion F and 14 others (2019) The Open Global Glacier Model (OGGM) v1.1. *Geoscientific Model Development* **12**(3), 909–931. doi:10.5194/gmd-12-909-2019

McNabb RW, Hock R and Huss M (2015) Variations in Alaska tidewater glacier frontal ablation, 1985–2013. *Journal of Geophysical Research: Earth Surface* **120**(1), 120–136. doi:10.1002/2014JF003276

McNabb RW and Hock R (2014) Alaska tidewater glacier terminus positions, 1948–2012. *Journal of Geophysical Research: Earth Surface* **119**(2), 153–167. doi:10.1002/2013JF002915
McNeil C and 6 others (2020) Explaining mass balance and retreat dichotomies at Taku and Lemon Creek Glaciers, Alaska. *Journal of Glaciology* **66**(258), 530–542. doi:10.1017/jog.2020.22
Minowa M, Schaefer M and Skvarca P (2023) Effects of topography on dynamics and mass loss of lake-terminating glaciers in southern Patagonia. *Journal of Glaciology* **69**(278), 1580–1597. doi:10.1017/jog.2023.42
Minowa M, Schaefer M, Sugiyama S, Sakakibara D and Skvarca P (2021) Frontal ablation and mass loss of the Patagonian icefields. *Earth and Planetary Science Letters* **561**, 116811. doi:10.1016/j.epsl.2021.116811
Mölg N and 7 others (2021) Inventory and evolution of glacial lakes since the Little Ice Age: Lessons from the case of Switzerland. *Earth Surface Processes and Landforms* **46**(13), 2551–2564. doi:10.1002/esp.5193
Mouginot J and 8 others (2019) Forty-six years of Greenland Ice Sheet mass balance from 1972 to 2018. *Proceedings of the National Academy of Sciences* **116**(19), 9239–9244. doi:10.1073/pnas.1904242116
Nick FM, Veen CJVD, Vieli A and Benn DI (2010) A physically based calving model applied to marine outlet glaciers and implications for the glacier dynamics. *Journal of Glaciology* **56**(199), 781–794. doi:10.3189/002214310794457344
Partington G (2023) Reconstructing the Surge History and Dynamics of Fisher Glacier, Yukon, 1948-2022. Université d'Ottawa / University of Ottawa. http://hdl.handle.net/10393/45084
Pfeffer WT (2007) A simple mechanism for irreversible tidewater glacier retreat.

References

Benn DI, Warren CR and Mottram RH (2007a) Calving processes and the dynamics of calving glaciers. *Earth-Science Reviews* **82**(3–4), 143–179. doi:10.1016/j.earscirev.2007.02.002
Benn DI, Hulton NRJ and Mottram RH (2007b) 'Calving laws', 'sliding laws' and the stability of tidewater glaciers. *Annals of Glaciology* **46**, 123–130. doi:10.3189/172756407782871161
Boyce ES, Motyka RJ and Truffer M (2007) Flotation and retreat of a lake-calving terminus, Mendenhall Glacier, southeast Alaska, USA. *Journal of Glaciology* **53**(181), 211–224. doi:10.3189/172756507782202928
Brown CS, Meier MF and Post A (1982) Calving speed of Alaska tidewater glaciers, with application to Columbia Glacier. *Professional Paper*. doi:10.3133/pp1258C
Burgess EW, Forster RR, Larsen CF and Braun M (2012) Surge dynamics on Bering Glacier, Alaska, in 2008–2011. *The Cryosphere* **6**(6), 1251–1262. doi:10.5194/tc-6-1251-2012
Carrivick JL and 7 others (2022) Coincident evolution of glaciers and ice-marginal proglacial lakes across the Southern Alps, New Zealand: Past, present and future. *Global and Planetary Change* **211**, 103792. doi:10.1016/j.gloplacha.2022.103792
Carrivick JL and Tweed FS (2013) Proglacial lakes: character, behaviour and geological importance. *Quaternary Science Reviews* **78**, 34–52. doi:10.1016/j.quascirev.2013.07.028
Chen F and 6 others (2021) Annual 30 m dataset for glacial lakes in High Mountain Asia from 2008 to 2017. *Earth System Science Data* **13**(2), 741–766. doi:10.5194/essd-13-741-2021
Cook SJ and Quincey DJ (2015) Estimating the volume of Alpine glacial lakes. doi:10.5194/esurfd-3-909-2015
Cuffey KM and Paterson WSB (2010) *The physics of glaciers.*, Fourth edition. Elsevier, San Diego.
Dorava JM and Milner AM (2000) Role of lake regulation on glacier-fed rivers in enhancing salmon productivity: the Cook Inlet watershed, south-central Alaska, USA. *Hydrological Processes* **14**(16–17), 3149–3159. doi:10.1002/1099-1085(200011/12)14:16/17<3149::AID-HYP139>3.0.CO;2-Y
Dye A, Bryant R, Dodd E, Falcini F and Rippin DM (2021) Warm Arctic Proglacial Lakes in the ASTER Surface Temperature Product. *Remote Sensing* **13**(15), 2987. doi:10.3390/rs13152987
European Space Agency (2024). *CopernicusGlobal Digital Elevation Model*. Distributed by OpenTopography. https://doi.org/10.5069/G9028PQB Accessed: 05/01/2023
Farinotti D, Round V, Huss M, Compagno L and Zekollari H (2019) Large hydropower and water-storage potential in future glacier-free basins. *Nature* **575**(7782), 341–344. doi:10.1038/s41586-019-1740-z
Gardner A, Fahnestock M and Scambos T (2022) MEaSUREs ITS_LIVE Regional Glacier and Ice Sheet Surface Velocities, Version 1. doi:10.5067/6II6VW8LLWJ7
Helsel DR, Hirsch RM, Ryberg KR, Archfield SA and Gilroy EJ (2020) Statistical methods in water resources. 4-A3. U.S. Geological Survey. doi:10.3133/tm4A3
How P and 10 others (2021) Greenland-wide inventory of ice marginal lakes using a multi-method approach. *Scientific Reports* **11**(1), 4481. doi:10.1038/s41598-021-83509-1
Hugonnet R and 10 others (2021) Accelerated global glacier mass loss in the early twenty-first century. *Nature* **592**(7856), 726–731. doi:10.1038/s41586-021-03436-z

https://doi.org/10.1017/jog.2025.37 Published online by Cambridge University Press

King O, Bhattacharya A, Bhambri R and Bolch T (2019) Glacial lakes exacerbate Himalayan glacier mass loss. *Scientific Reports* **9**(1), 18145. doi:10.1038/s41598-019-53733-x
Kochtitzky W and 17 others (2022) The unquantified mass loss of Northern Hemisphere marine-terminating glaciers from 2000–2020. *Nature Communications* **13**(1), 5835. doi:10.1038/s41467-022-33231-x
Larsen CF, Burgess E, Arendt AA, O'Neel S, Johnson AJ and Kienholz C (2015) Surface melt dominates Alaska glacier mass balance. *Geophysical Research Letters* **42**(14), 5902–5908. doi:10.1002/2015GL064349
Lea JM (2018) The Google Earth Engine Digitisation Tool (GEEDiT) and the Margin change Quantification Tool (MaQiT) – simple tools for the rapid mapping and quantification of changing Earth surface margins. *Earth Surface Dynamics* **6**(3), 551–561. doi:10.5194/esurf-6-551-2018
Main B and 11 others (2023) Terminus change of Kaskawulsh Glacier, Yukon, under a warming climate: retreat, thinning, slowdown and modified proglacial lake geometry. *Journal of Glaciology* **69**(276), 936–952. doi:10.1017/jog.2022.114
Maurer JM, Schaefer JM, Rupper S and Corley A (2019) Acceleration of ice loss across the Himalayas over the past 40 years. *Science Advances* **5**(6), eaav7266. doi:10.1126/sciadv.aav7266
Maussion F and 14 others (2019) The Open Global Glacier Model (OGGM) v1.1. *Geoscientific Model Development* **12**(3), 909–931. doi:10.5194/gmd-12-909-2019
McNabb RW, Hock R and Huss M (2015) Variations in Alaska tidewater glacier frontal ablation, 1985–2013. *Journal of Geophysical Research: Earth Surface* **120**(1), 120–136. doi:10.1002/2014JF003276
McNabb RW and Hock R (2014) Alaska tidewater glacier terminus positions, 1948–2012. *Journal of Geophysical Research: Earth Surface* **119**(2), 153–167. doi:10.1002/2013JF002915
McNeil C and 6 others (2020) Explaining mass balance and retreat dichotomies at Taku and Lemon Creek Glaciers, Alaska. *Journal of Glaciology* **66**(258), 530–542. doi:10.1017/jog.2020.22
Minowa M, Schaefer M and Skvarca P (2023) Effects of topography on dynamics and mass loss of lake-terminating glaciers in southern Patagonia. *Journal of Glaciology* **69**(278), 1580–1597. doi:10.1017/jog.2023.42
Minowa M, Schaefer M, Sugiyama S, Sakakibara D and Skvarca P (2021) Frontal ablation and mass loss of the Patagonian icefields. *Earth and Planetary Science Letters* **561**, 116811. doi:10.1016/j.epsl.2021.116811
Mölg N and 7 others (2021) Inventory and evolution of glacial lakes since the Little Ice Age: Lessons from the case of Switzerland. *Earth Surface Processes and Landforms* **46**(13), 2551–2564. doi:10.1002/esp.5193
Mouginot J and 8 others (2019) Forty-six years of Greenland Ice Sheet mass balance from 1972 to 2018. *Proceedings of the National Academy of Sciences* **116**(19), 9239–9244. doi:10.1073/pnas.1904242116
Nick FM, Veen CJVD, Vieli A and Benn DI (2010) A physically based calving model applied to marine outlet glaciers and implications for the glacier dynamics. *Journal of Glaciology* **56**(199), 781–794. doi:10.3189/002214310794457344
OpenTopography (2021) Copernicus GLO-90 Digital Surface Model. doi:10.5069/G9028PQB
Partington G (2023) Reconstructing the Surge History and Dynamics of Fisher Glacier, Yukon, 1948-2022. Université d'Ottawa / University of Ottawa. http://hdl.handle.net/10393/45084
Pfeffer WT (2007) A simple mechanism for irreversible tidewater glacier retreat. *Journal of Geophysical Research: Earth Surface* **112**(F3). doi:10.1029/2006JF000590
Post A, O'Neel S, Motyka RJ and Streveler G (2011) A complex relationship between calving glaciers and climate. *Eos, Transactions American Geophysical Union* **92**(37), 305–306. doi:10.1029/2011EO370001
Pronk JB, Bolch T, King O, Wouters B and Benn DI (2021) Contrasting surface velocities between lake- and land-terminating glaciers in the Himalayan region. *The Cryosphere* **15**(12), 5577–5599. doi:10.5194/tc-15-5577-2021
Recinos B, Maussion F, Rothenpieler T and Marzeion B (2019) Impact of frontal ablation on the ice thickness estimation of marine-terminating glaciers in Alaska. *The Cryosphere* **13**(10), 2657–2672. doi:10.5194/tc-13-2657-2019
RGI Consortium (2017) Randolph Glacier Inventory - A Dataset of Global Glacier Outlines, Version 6. doi:10.7265/4M1F-GD79
Rick B, McGrath D, Armstrong W and McCoy SW (2022) Dam type and lake location characterize ice-marginal lake area change in Alaska and NW Canada between 1984 and 2019. *The Cryosphere* **16**(1), 297–314. doi:10.5194/tc-16-297-2022
Rignot E, Mouginot J, Scheuchl B, van den Broeke M, van Wessem MJ and Morlighem M (2019) Four decades of Antarctic Ice Sheet mass balance from 1979–2017. *Proceedings of the National Academy of Sciences* **116**(4), 1095–1103. doi:10.1073/pnas.1812883116

Robertson CM, Benn DI, Brook MS, Fuller lan C and Holt KA (2012) Subaqueous calving margin morphology at Mueller, Hooker and Tasman glaciers in Aoraki/Mount Cook National Park, New Zealand. *Journal of Glaciology* **58**(212), 1037–1046. doi:10.3189/2012JoG12J048

Shugar DH and 9 others (2020) Rapid worldwide growth of glacial lakes since 1990. *Nature Climate Change* **10**(10), 939–945. doi:10.1038/s41558-020-0855-4

Sugiyama S, Minowa M and Schaefer M (2019) Underwater Ice Terrace Observed at the Front of Glaciar Grey, a Freshwater Calving Glacier in Patagonia. *Geophysical Research Letters* **46**(5), 2602–2609. doi:10.1029/2018GL081441

Sugiyama S and 7 others (2016) Thermal structure of proglacial lakes in Patagonia. *Journal of Geophysical Research: Earth Surface* **121**(12), 2270–2286. doi:10.1002/2016JF004084

Tangborn W (2013) Mass balance, runoff and surges of Bering Glacier, Alaska. *The Cryosphere* **7**(3), 867–875. doi:10.5194/tc-7-867-2013

Tober BS (2023) Radar Sounding Analysis of Mountain Glaciers in Alaska: Revealing Ice Thickness, Subglacial Topography, and Geologic Structure. https://repository.arizona.edu/handle/10150/668124

Truffer M and Motyka RJ (2016) Where glaciers meet water: Subaqueous melt and its relevance to glaciers in various settings. *Reviews of Geophysics* **54**(1), 220–239. doi:10.1002/2015RG000494

Trüssel BL, Motyka RJ, Truffer M and Larsen CF (2013) Rapid thinning of lake-calving Yakutat Glacier and the collapse of the Yakutat Icefield, southeast Alaska, USA. *Journal of Glaciology* **59**(213), 149–161. doi:10.3189/2013J0G12J081

Tsutaki S, Nishimura D, Yoshizawa T and Sugiyama S (2011) Changes in glacier dynamics under the influence of proglacial lake formation in Rhonegletscher, Switzerland. *Annals of Glaciology* **52**(58), 31–36. doi:10.3189/172756411797252194

Warren CR and Kirkbride MP (2003) Calving speed and climatic sensitivity of New Zealand lake-calving glaciers. *Annals of Glaciology* **36**, 173–178. doi:10.3189/172756403781816446

Welty E and 12 others (2020) Worldwide version-controlled database of glacier thickness observations. *Earth System Science Data* **12**(4), 3039–3055. doi:10.5194/essd-12-3039-2020

Wilson R and 6 others (2018) Glacial lakes of the Central and Patagonian Andes. *Global and Planetary Change* **162**, 275–291. doi:10.1016/j.gloplacha.2018.01.004

Yang R and 6 others (2022) Glacier Surface Speed Variations on the Kenai Peninsula, Alaska, 2014–2019. *Journal of Geophysical Research: Earth Surface* **127**(3), e2022JF006599. doi:10.1029/2022JF006599

Zemp M and 14 others (2019) Global glacier mass changes and their contributions to sea-level rise from 1961 to 2016. *Nature* **568**(7752), 382–386. doi:10.1038/s41586-019-1071-0

Zhang G and 12 others (2024) Characteristics and changes of glacial lakes and outburst floods. *Nature Reviews Earth & Environment* **5**(6), 447–462. doi:10.1038/s43017-024-00554-w

Zhang G and 9 others (2023) Underestimated mass loss from lake-terminating glaciers in the greater Himalaya. *Nature Geoscience* **16**(4), 333–338. doi:10.1038/s41561-023-01150-1

ournal of Geophysical Research: Earth Surface **112**(F3). doi:10.1029/2006JF000590

Post A, O'Neel S, Motyka RJ and Streveler G (2011) A complex relationship between calving glaciers and climate. *Eos, Transactions American Geophysical Union* **92**(37), 305–306. doi:10.1029/2011EO370001

Pronk JB, Bolch T, King O, Wouters B and Benn DI (2021) Contrasting surface velocities between lake- and land-terminating glaciers in the Himalayan region. *The Cryosphere* **15**(12), 5577–5599. doi:10.5194/tc-15-5577-2021

Recinos B, Maussion F, Rothenpieler T and Marzeion B (2019) Impact of frontal ablation on the ice thickness estimation of marine-terminating glaciers in Alaska. *The Cryosphere* **13**(10), 2657–2672. doi:10.5194/tc-13-2657-2019

RGI Consortium (2017) Randolph Glacier Inventory - A Dataset of Global Glacier Outlines, Version 6. doi:10.7265/4M1F-GD79

Rick B, McGrath D, Armstrong W and McCoy SW (2022) Dam type and lake location characterize ice-marginal lake area change in Alaska and NW Canada between 1984 and 2019. *The Cryosphere* **16**(1), 297–314. doi:10.5194/tc-16-297-2022

Rignot E, Mouginot J, Scheuchl B, van den Broeke M, van Wessem MJ and Morlighem M (2019) Four decades of Antarctic Ice Sheet mass balance from 1979–2017. *Proceedings of the National Academy of Sciences* **116**(4), 1095–1103. doi:10.1073/pnas.1812883116

Robertson CM, Benn DI, Brook MS, Fuller lan C and Holt KA (2012) Subaqueous calving margin morphology at Mueller, Hooker and Tasman glaciers in Aoraki/Mount Cook National Park, New Zealand. *Journal of Glaciology* **58**(212), 1037–1046. doi:10.3189/2012JoG12J048

https://doi.org/10.1017/jog.2025.37 Published online by Cambridge University Press

Shugar DH and 9 others (2020) Rapid worldwide growth of glacial lakes since 1990. *Nature Climate Change* **10**(10), 939–945. doi:10.1038/s41558-020-0855-4

Sugiyama S, Minowa M and Schaefer M (2019) Underwater Ice Terrace Observed at the Front of Glaciar Grey, a Freshwater Calving Glacier in Patagonia. *Geophysical Research Letters* **46**(5), 2602–2609. doi:10.1029/2018GL081441

Sugiyama S and 7 others (2016) Thermal structure of proglacial lakes in Patagonia. *Journal of Geophysical Research: Earth Surface* **121**(12), 2270–2286. doi:10.1002/2016JF004084

Tangborn W (2013) Mass balance, runoff and surges of Bering Glacier, Alaska. *The Cryosphere* **7**(3), 867–875. doi:10.5194/tc-7-867-2013

Tober BS (2023) Radar Sounding Analysis of Mountain Glaciers in Alaska: Revealing Ice Thickness, Subglacial Topography, and Geologic Structure. https://repository.arizona.edu/handle/10150/668124

Truffer M and Motyka RJ (2016) Where glaciers meet water: Subaqueous melt and its relevance to glaciers in various settings. *Reviews of Geophysics* **54**(1), 220–239. doi:10.1002/2015RG000494

Trüssel BL, Motyka RJ, Truffer M and Larsen CF (2013) Rapid thinning of lake-calving Yakutat Glacier and the collapse of the Yakutat Icefield, southeast Alaska, USA. *Journal of Glaciology* **59**(213), 149–161. doi:10.3189/2013J0G12J081

Tsutaki S, Nishimura D, Yoshizawa T and Sugiyama S (2011) Changes in glacier dynamics under the influence of proglacial lake formation in Rhonegletscher, Switzerland. *Annals of Glaciology* **52**(58), 31–36. doi:10.3189/172756411797252194

Warren CR and Kirkbride MP (2003) Calving speed and climatic sensitivity of New Zealand lake-calving glaciers. *Annals of Glaciology* **36**, 173–178. doi:10.3189/172756403781816446

Welty E and 12 others (2020) Worldwide version-controlled database of glacier thickness observations. *Earth System Science Data* **12**(4), 3039–3055. doi:10.5194/essd-12-3039-2020

Wilson R and 6 others (2018) Glacial lakes of the Central and Patagonian Andes. *Global and Planetary Change* **162**, 275–291. doi:10.1016/j.gloplacha.2018.01.004

Yang R and 6 others (2022) Glacier Surface Speed Variations on the Kenai Peninsula, Alaska, 2014–2019. *Journal of Geophysical Research: Earth Surface* **127**(3), e2022JF006599. doi:10.1029/2022JF006599

Zemp M and 14 others (2019) Global glacier mass changes and their contributions to sea-level rise from 1961 to 2016. *Nature* **568**(7752), 382–386. doi:10.1038/s41586-019-1071-0

Zhang G and 12 others (2024) Characteristics and changes of glacial lakes and outburst floods. *Nature Reviews Earth & Environment* **5**(6), 447–462. doi:10.1038/s43017-024-00554-w

Zhang G and 9 others (2023) Underestimated mass loss from lake-terminating glaciers in the greater Himalaya. *Nature Geoscience* **16**(4), 333–338. doi:10.1038/s41561-023-01150-1